VOL. 9 No. 12, pp. 349-380 1947/1948

Philips Technical Review

DEALING WITH TECHNICAL PROBLEMS
RELATING TO THE PRODUCTS, PROCESSES AND INVESTIGATIONS OF
THE PHILIPS INDUSTRIES

EDITED BY THE RESEARCH LABORATORY OF N.V. PHILIPS' GLOEILAMPENFABRIEKEN, EINDHOVEN, NETHERLANDS.

THE MANUFACTURE OF CORRECTION PLATES FOR SCHMIDT OPTICAL SYSTEMS

by H. RINIA and P. M. van ALPHEN.

535.313

When an image is formed with optical systems employing mirrors or lenses, the imperfect imaging due to aberrations often gives rise to great difficulties. Disregarding those of a higher order, there are five defects: the spherical aberration, coma, astigmatism, curvature of the field and distortion. In 1931 B. Schmidt designed a mirror system which is corrected very well for four of these five defects, whilst the influence of the curvature of the field upon the distortion may usually be ignored. Schmidt introduced a diaphragm and a correction plate in the centre of curvature of a spherical mirror. The great advantage of this system lies in the fact that it allows of large apertures being used while giving at the same time a reasonably large useful field of vision. First the working of this Schmidt optical system and the shape of the correction plate will be discussed, followed by a description of a new method worked out in the Philips laboratory at Eindhoven for the manufacture of these correction plates. With this method a mould is used the face of which is the negative of the plate required, but with the thickness dimensions exaggerated, for instance, five times. A 20% gelatin solution is then applied on the mould and after it has dried it shows the desired shape. Schmidt's system, first applied in astronomical telescopes, is also useful for various other optical purposes.

Introduction

Most optical instruments are designed to produce an image of an object. This image sometimes has to be enlarged, as in the case of projection lenses, or reduced, as in the case of photographic lenses but it is always required to be sharp and conformable to the object. That it is not so simple to meet this requirement is apparent from the fact that astronomical telescopes, used for producing an image of a celestial constellation, have already taken more than three centuries to develop and still cannot be said to be perfect. Aberrations still cause a certain unsharpness of the images and lack of conformity with the object.

The principal aberrations have been dealt with in an article published in a previous issue of this journal [1]), where it was shown that their magnitude depends upon the distance y_0 from the paraxial image point to the optical axis of the system and upon the height of incidence H of the light ray.

If we confine ourselves to third order aberrations, i.e. those which are proportional to at most the third power of the parameters just mentioned, then, when using monochromatic light, there are five optical aberrations: spherical aberration, coma, astigmatism, curvature of the field and distortion. When we work with composite light then in addition to these five defects we have to contend with two chromatic aberrations.

Optical systems have been constructed in various ways in an attempt to eliminate these aberrations as far as possible. In astronomical reflectors, for instance, the hollow mirror has been made parabolic instead of spherical. When stars are observed in the axial direction no aberrations then occur even when the height of incidence H is great, but when there are pencils of rays making an angle with the axis then coma and astigmatism very soon lead to large aberrations, with a parabolic mirror a large aperture can, in fact, be used but the field of vision is small.

Another possibility is that with a spherical mirror a diaphragm is placed in the centre of cur-

[1]) W. de Groot, Optical Aberrations in lens and mirror systems. Philips Techn. Rev. 9, 301-307, 1947 (No. 10).

vature. In directions making a fairly large angle with the optical axis of the system some of the aberrations are avoided, just as is the case in the direction of the axis, but the spherical aberration remains. In order to limit the effect of this spherical aberration it is necessary to give the diaphragm a small aperture; in the case of a spherical mirror with the diaphragm in the centre of curvature one can work with a large field of vision, but one must then make the aperture small, and this means low luminous intensity.

With lens systems attemps have been made to eliminate aberrations by combining lenses of different shapes and different kinds of glass. Thus composite lenses are formed which eliminate certain aberrations. But for an optical system with large aperture and large field of vision it is impossible to correct all aberrations at once in this way. Often the elimination of some aberrations is accompanied by a greater effect of the others. It is particularly the aberrations of higher orders that then play a part. Even if a lens system were designed in such a way that all third order aberrations of one part were absolutely neutralized by the corresponding aberrations of the other part, there would still be no guarantee that the image is sharp. Aberrations of the fifth and higher orders may still completely spoil the image. It is impossible to suppress these aberrations exactly together with those of lower

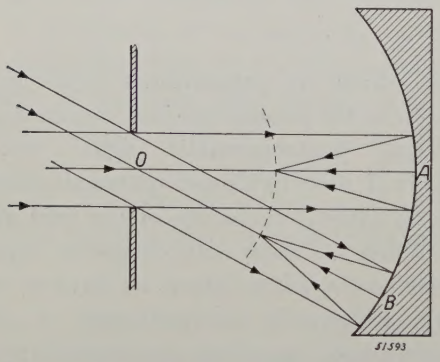

Fig. 1. A spherical hollow mirror with a diaphragm in a plane passing through the centre of curvature O. The images formed by the beams with parallel rays A and B lie on a spherical surface with $^1/_2 R$ as radius, R representing the radius of the mirror and O its centre.

orders. The greater the parameters y_0 and H, *i.e.* the larger the field of vision and the higher the luminous intensity, the greater is the effect of these higher order aberrations.

An important construction designed with the object of correcting aberrations as far as possible while retaining a large field of vision and extremely high luminous intensity is Schmidt's mirror system. In the article quoted in footnote [1]) it has already been stated that in this system a spherical hollow mirror and a correction plate with an aspherical surface are used.

In the present article a new method is described for the manufacture of these plates, a method which has been worked out in the Philips laboratory at Eindhoven. First, however, we shall discuss briefly the working of this Schmidt optical system and the shape of the correction plate.

B. Schmidt's invention

B. Schmidt, an instrument-maker of the Hamburg Observatory at Bergedorf, invented his optical system in 1931. We shall consider the points he had in mind when devising this system [2]).

Schmidt started with a spherical hollow mirror. This offers at once two great advantages. In the first place a mirror is perfectly free of all chromatic aberrations, and further, given equal focal distance and diameter, the spherical aberration of a hollow mirror is eight times smaller than that of a simple lens.

In the centre of the spherical mirror (the radius of which we shall call R) Schmidt placed a diaphragm. Since the direction of each incident ray can now be regarded as the optical axis, the coma and astigmatism related to the diaphragm plane are nil. The image field for beams of parallel rays is a part of a sphere with $^1/_2 R$ as radius, as is seen in *fig. 1*. For photographic telescopes and various other purposes (screen photography, projectors for television receivers) the fact that we have to do with a curved image field does not constitute any great objection,for the film or the screen of the cathode-ray tube can be made spherical, so that this curvature of the field is of no effect. If with a hollow mirror a diaphragm is placed in the centre of curvature and a spherical image field is used, then all aberrations except the spherical aberration are eliminated, not only those of the third order but also those of higher orders.

Strictly speaking, there is still the effect of distortion. Since this defect is independent of the diaphragm aperture it does not disappear even when the aperture is made small to counteract spherical aberration.

This occurrence of distortion is apparently contradictory to what has been stated in the article quoted in footnote [1]) about the value of the coefficients $c_1 \ldots c_4$ governing the third order aberrations. There it is argued that in our case the coefficient c_4 is nil, from which it is to be concluded that no distortion occurs. It must be borne in mind, however, that the coefficients $c_1, \ldots c_4$ relate to the intersection of the ray in question on a flat plane perpendicular to the axis in the focal point. The secondary axis ($H = 0$) does indeed intersect

[2]) Central-Zeitung für Optik and Mechanik, **52**, No. 2, 1931.

this plane, after reflection, at the point $y_0 = {}^1/_2\ R \tan \vartheta$, where y_0 represents the position of the paraxial image field and ϑ the angle between the secondary axis in question and the main axis. When, however, we have a curved image field (a sphere with radius ${}^1/_2\ R$) and consider the point where the same ray intersects this sphere, then the distance from this point of intersection to the axis measured along the sphere is ${}^1/_2\ R\ \vartheta$, and since $\vartheta = t - {}^1/_3\ t^3$ when $t = \tan \vartheta$ this may be regarded as a distortion, which becomes manifest, for instance, when a strip of film originally stretched over the surface of the sphere is laid out flat and we examine the image in this spherical surface drawn out flat. As a rule, however, this distortion is so slight that its influence may be ignored.

The only image defect that has to be eliminated is the spherical aberration. Schmidt does this by introducing a correction plate in the diaphragm.

The manner in which this correction element works can be explained with reference to *fig. 2*. We assume that a source of light is placed in the focus of a hollow spherical mirror. In the top half of the drawing it is shown how the rays coming from the focus are reflected when there is no correction plate. Only the paraxial rays run practically parallel to the main axis after reflection. The greater the angle between the incident ray and the main axis, the more the reflected ray diverges from the line parallel to the main axis.

In the bottom half of the illustration it is indicated how Schmidt has eliminated this spherical aberration. We can imagine that owing to the refraction in a prismatic piece of glass each of the reflected rays is made to run parallel to the major axis of the mirror. All these glass prisms together then form the correction element. The division into a large number of very thin prisms is only a schematic representation. Actually the correction plate has a continuous surface. In the illustration the thickness of this plate is greatly magnified.

Schmidt realized that it is of great importance to apply the correction plate in the centre of the mirror. This gives the same great advantage as mentioned above when the diaphragm is placed in that centre. Since all the incident rays now bear the same relations in respect to the correction element, when constructing the passage of the rays through this element one may regard each direction as the optical axis. In regard to the rays not passing along the main axis of the mirror, the correction plate is not, it is true, perpendicular to the direction of incidence, but since the deflection of a ray through a prismatic piece of glass is only to a very small extent dependent upon the angle of incidence, the differences thereby arising may be regarded as an effect of a higher order.

This is more readily understood when it is borne in mind that the purpose of introducing the plate in the diaphragm is only to correct the image. The correction element is very thin, the optical strength of the system being supplied by the hollow mirror. When owing to the angle of incidence the direction of the non-paraxial rays is slightly

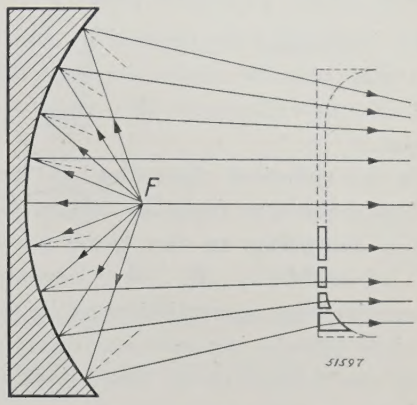

Fig. 2. The effect of a correction plate applied to a spherical hollow mirror. A light source is imagined as being situated in the focus F of the mirror. The top half of the figure shows the direction given to the reflected rays as a consequence of spherical aberration. The bottom half shows how a correction plate bends the reflected rays into a parallel beam.

changed in the correction plate, this only results in a change in the correction, in contrast to the case of a lens system where the angle of incidence of the boundary rays causes these to pass through an entirely different thickness of glass, resulting directly in a change in the image. That is why a Schmidt optical system can be used with an aperture much larger in relation to the focal distance than is the case with a lens system.

There is one other point that must be briefly dealt with here. It has been stated above that with a hollow mirror no chromatic aberrations occur. But as the correction plate refracts, it has dispersion and consequently gives different deviations to rays of different wavelengths. This can be taken into account when deciding upon the shape of the correction plate, taking care to keep the influence of chromatic aberration as small as possible. Consideration must also be given to the fact that the difference in cross section between the thickest and the thinnest part of the correction plate is very small, often not more than a few tenths of a millimeter, so that there need be no fear of any appreciable effect of chromatic aberration with a plate such as this.

With a parabolic mirror the spherical aberration is eliminated in only one direction, whereas with Schmidt's mirror system it is practically eliminated in all directions. Since also the other

aberrations (except for the curvature of the field) are practically eliminated for all directions, this optical system can be used with a large aperture and moreover has a fairly large field of vision.

All we have to do is to construct a correction plate that meets all the requirements.

The shape of the correction plate

Before discussing the method by which the correction plate can be made, we shall first show a simple way to calculate the required shape of the plate.

Since the spherical aberration — the angle of deviation of the rays from the desired direction — increases according to the third power of the height of incidence H, the correction plate compensating this aberration must have a surface whose slope likewise increases according to the third power of the distance to the axis. With a prism the deviation is proportional to the angle of refraction. The thickness of the correction plate (one side of which is imagined as being flat) must therefore increase from the middle in proportion to H^4. If also fifth and seventh order aberrations are taken into account, then the thickness of the plate must conform to the equation

$$d = d_0 + BH^4 + CH^6 + DH^8, \ldots \quad (1)$$

where B, C and D are still unknown coefficients.

From this formula it follows — as already appears from the construction of the passage of the rays in fig. 2 — that in the middle the correction plate has to be very flat, rapidly increasing in thickness towards the edge.

It is advantageous to reduce the difference in thickness between the middle and the edge of the plate, for it has been seen above that the correction element gives rise to two kinds of aberrations: 1) chromatic aberrations due to dispersion, and 2) aberrations due to the angle of incidence of the non-paraxial rays. These aberrations can be reduced by making the absolute value of the deviation as small as possible. One must not, therefore, use the form of plate schematically represented in fig. 2, which shows a very large slope at the edge while the middle is practically flat. Instead we have to construct a plate in such a way that the slope at the edge is reduced by giving the surface in the middle a slope in the opposite direction. This can be achieved by adding to formula (1) a term $-AH^2$ (A positive), so that we get the expression:

$$d = d_0 - AH^2 + BH^4 + CH^6 + DH^8. \quad (2)$$

In this manner the correction plate is applied as it were to a flat-spherical lens. *Fig. 3* shows side by side the original correction plate, this flat-spherical lens and the plate obtained by a combination of the first two. The thickness and the slope at the edge have thereby been reduced, whilst the flat minimum in the thickness has been shifted from the middle to close to the edge. The rays passing through this zone of the minimum are not refracted. The point where after reflection from the hollow mirror they intersect the axis has now become the point where all the rays converge.

Owing to the addition of the flat-spherical lens the focal distance of the system is somewhat lengthened, as will be found when following the passage of the paraxial rays, but there is no objection to this.

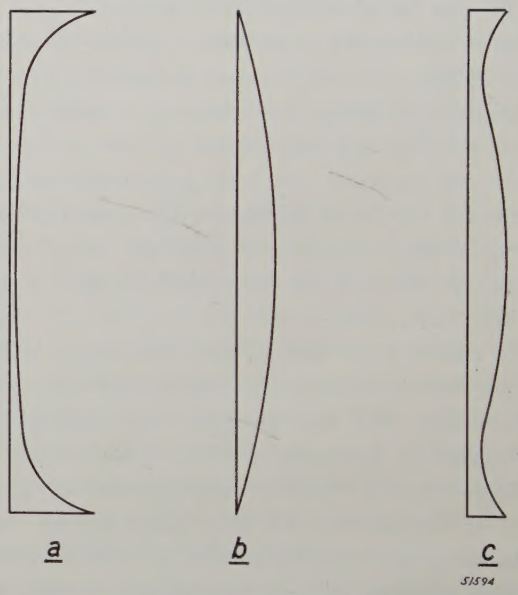

Fig. 3. *a*) A correction plate for a Schmidt optical system. *b*) A flat-spherical lens with which the correction plate is often combined.
c) The shape that the correction plate assumes when combined with *b*.
The thickness of the plate is strongly exaggerated in these illustrations.

The coefficients A, B, C and D and d_0 in formula (2) are determined by calculating for a number of heights of incidence H the value required of the slope and thus of the thickness of the plate.

Fig. 4 shows diagrammatically how the correction plate in its ultimate form causes the rays of a parallel beam to converge upon one point after reflection from a hollow mirror.

The effect of the correction plate is also clearly seen from the two photographs reproduced in *fig. 5*, likewise relating to a pencil of parallel rays reflected by a hollow mirror. In fig. 5*a* there is spherical aberration, whilst in fig. 5*b* this has been eliminated by means of a correction plate.

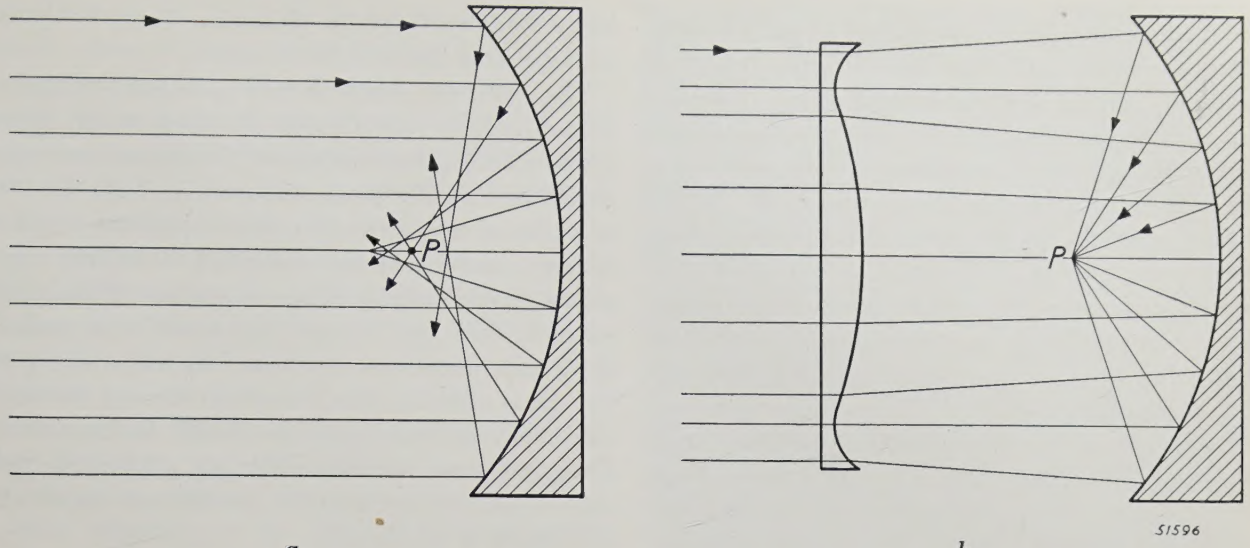

a *b*

Fig. 4. *a*) With a spherical mirror the rays of the beams at different distances from the optical axis converge at different points.
b) The effect of the correction plate is to cause all parallel rays to converge at one and the same focal point *P*.

The manufacture of the correction plate

Having determined the shape that the correction plate should have, we must then consider the question how to make a plate conforming exactly to that shape.

Schmidt used a plate of glass, but the correction element may also be made of any other transparent and light-refracting substance.

When Schmidt published his invention he did not say how he gave the correction plate the right shape. Many believed that the grinding of such a plate would cost hundreds of hours of work and that this would be an objection against the application of this new construction in practice.

After Schmidt's death in 1935, R. Schorr published the method employed by this Hamburg instrument maker [3]). It then appeared that Schmidt had been making his correction plates in an ingenious manner without it costing him too much time. He had realized that the curved plane of the correction plate corresponded approximately

[3]) Zeitschrift für Instrumentkunde, **56**, 336-338, 1936.

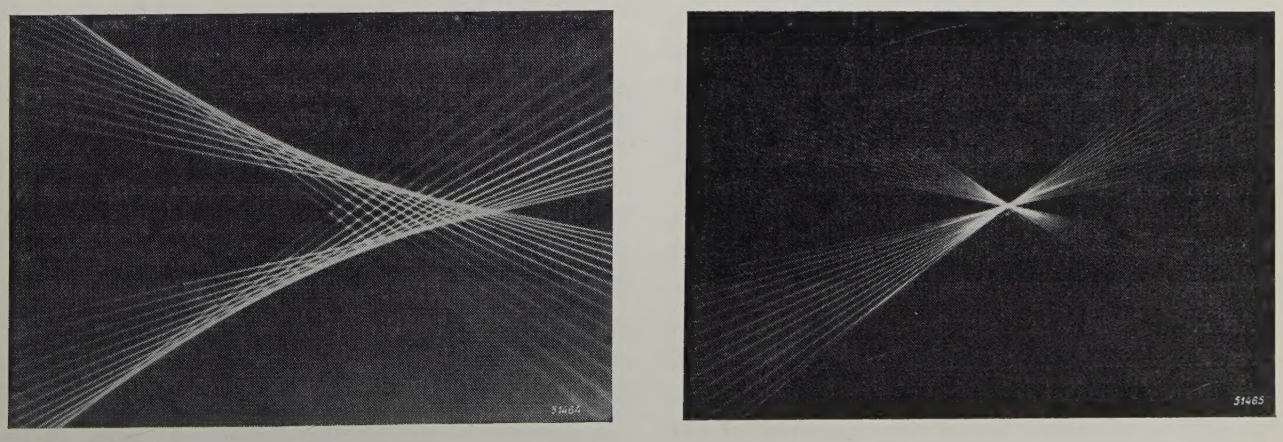

a *b*

Fig. 5. The influence of a correction plate on the passage of rays reflected from a spherical hollow mirror. *a*) The course followed by the rays without the correction plate. On the left is the hollow mirror reflecting the rays, which are made visible here. *b*) The course of the rays when a correction plate is used. Before striking the mirror the rays pass through a correction plate. The rays which in *a*) form an extensive caustic curve converge in *b*) upon a sharply defined focal point. These photographs were taken with a slanting photographic plate in the focus of the mirror system. In both cases the central rays of the beam reflected by the mirror have been blocked out.

to the deflection plane that a circular plan-parallel plate supported round its edge assumes under a uniformly distributed pressure. Putting this into practical application, he laid a flat glass plate on the rim of a round vessel which he then evacuated until the necessary deflection took place. Schmidt then ground the upper surface of the glass plate in the deflected state until it was absolutely level. When he then let air flow into the vessel again, the ground surface assumed approximately the shape that it has to have for the boundary of the correction plate.

It is indeed a very ingeneous method, but A. Couder [4]) has proved that it is certainly not the right way for correction plates of small dimensions. And for large plates, such as are used for astronomical telescopes, this method is not accurate and is also rather cumbersome.

Various people have been investigating the ways and means of constructing these plates. Some have been hand-ground, in the same way as the parabolic mirror is made for a telescope, checking step by step in how far the desired result is reached and where improvements are still necessary. This method may be practicable for making one single plate for an astronomer's telescope, but it is certainly not suitable for the mass production which further technical applications require.

Another method is based on the use of transparent masses shaped in moulds under pressure, some plastic mass, for instance polystyrene, being pressed in a mould made in the desired shape. The mould has to be extremely accurate and have a surface of "optical quality". Moreover, it has to be able to withstand pressure or heating, so that the choice of material is limited. The mould is generally made and polished by hand and needs touching up in places to give it the right shape. A separate mould is thus needed for every correction plate of a different shape.

A new method for the manufacture of correction plates

An entirely new method for the manufacture of correction plates has been worked out at Eindhoven. On a turner's precision lathe a metal mould is made the surface of which forms the negative of the shape of the plate required. In the transversal directions the shape of this mould is of the same dimensions as the correction plate is required to have, but the differences in thickness are exaggerated about five times; if the actual correction plate has a total variation in thickness of say 0.5 mm, in the mould this will be 2.5 mm.

The carefully finished and polished mould is heated to abt. 40° C with running water, after which a 20% gelatin solution [5]) is poured onto the mould and a glass plate laid over it. With the aid of a pair of set-screws this plate is kept at a small distance away from the surface of the mould, any excess gelatin thereby being pressed out. When cold water is then run through the mould it is cooled down and the gelatin very soon sets into a stiff gel. The glass plate is then raised by turning the set-screws and removed from the mould. Owing to the strong adhesion between glass and gelatin the gel easily comes away from the mould and shows all the details of the mould.

The skin of gelatin is then hardened in formalin vapour and uniformly dried. Being held in the lateral directions by the glass plate, the gel shrinks only in thickness. The original surface is reduced in one direction, otherwise remaining unchanged. When a 20% gelatin solution is used 80% water

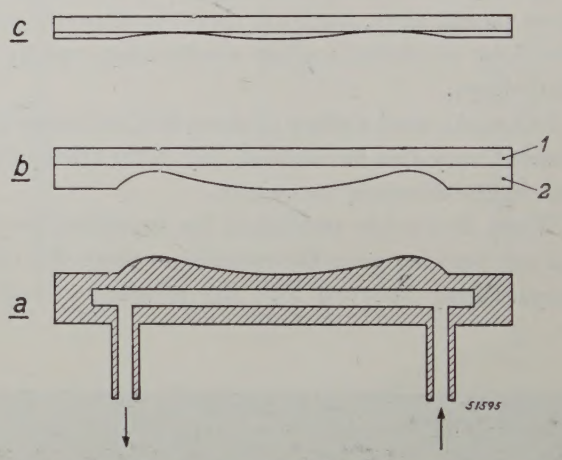

Fig. 6. *a*) A mould for a correction plate shown in cross section. This is a hollow mould with inlets and outlets for passing through cold or hot water.
b) A correction plate with layer of gelatin before drying. *1* represents the plan-parallel glass plate and *2* the layer of gelatin solution.
c) The same correction plate after drying.
In these illustrations the dimensions in the direction perpendicular to the correction plate have been greatly magnified.

will evaporate, leaving a glass plate covered with a thin layer of gelatin the surface of which is a five-fold reduction of that of the mould, thus exactly the required shape of the correction plate. It is astonishing how extremely accurate and uniform this shrinking is, producing a very smooth surface with every detail of the mould reduced five times

[4]) Comptes Rendus Ac. Sc. Paris **210**, 327-328, 1940.

[5]) This 20% gelatin solution is used when the differences in thickness in the mould are five times exaggerated. Other concentrations may be used, for instance a 10% solution, when the dimensions of thickness in the mould are exaggerated 10 times. See also footnote 6).

but otherwise true to shape. It is essential that the gelatin shows a really smooth surface after drying.

Fig. 6 shows a mould and also a correction plate before and after the drying of the gelatin. It will be understood that the dimensions in the direction perpendicular to the plate are greatly exaggerated in these drawings.

The hardened layer of gelatin is found to be very stable. Nevertheless, it may be advisable to protect the curved surface of the correction plate with a second flat glass plate, because wet fingers or drops of water are apt to damage the gelatin.

The method described offers a numbers of advantages over those applied hitherto:

1) Since the surface ultimately obtained is a fivefold reduction of the shape of the mould, the latter may be five times less accurate. If, for instance, the final shape is required to be accurate within 0.5 μ then the shape of the mould need only be accurate to within 2.5 μ. Any fine scratches in the mould are of no consequence, because these are also reduced five times when the gelatin dries; in many cases their depth becomes smaller than the wavelength of light, so that they become practically invisible.
2) The mould needs only moderate heating and cooling. Since there is no pressing there is no distortion arising therefrom.
3) Since the correction plate consists mainly of glass any distortion or mechanical deflection of the plate is precluded. The hardened layer of gelatin is highly impervious to scratching, so that the plate can safely be cleaned with a soft cloth.
4) Correction plates of different optical strengths can be made with one and the same mould, for one is not restricted to the concentration of 0.2 or 0.1. By varying the concentration of the gelatin solution one gets correction plates, after hardening, of different strength [6]).

Applications of the Schmidt optical system

Schmidt's first spherical mirror with correction plate was made for the Hamburg observatory. It was undoubtedly astronomy that he first had in mind as the field of application for his invention,

Fig. 7. Part of the Orion constellation as photographed in the Philips laboratory at Eindhoven when using a Schmidt mirror system (focal distance 8 cm) with a correction plate of gelatin. This photo demonstrates the large useful field of vision. Although its diameter is about 20° the image is sharp and free of aberrations right up to the edges of the photo.

and astronomers have in fact made good use of it. On January 1st 1941 there were already 44 observatories equipped with a Schmidt camera [7]). The great luminous intensity and extensive field of vision of these instruments have been turned to good advantage.

The aperture ratio of these cameras — that is to say the ratio of the diameter D of the objective to its focal distance F — shows clearly enough how great the improvement is in luminous intensity. When D/F is small one speaks of "slow" telescopes, because a long exposure time is required for making photographs. In the case of many previously built reflectors and refractors $D = F$: 5, F : 6 or F : 8, and sometimes still smaller. An exceptionally "rapid" telescope is the 200 inch telescope of Mount Palomar Observatory with $D = F$: 3.3.

But with the Schmidt optical systems the relative aperture is much greater. An astronomical camera with $D=F$:1 is quite a common type. Such a camera has a useful field of 25°, whilst the field of a parabolic telescope having an aperture equal to the focal distance would have to be measured in minutes. And cameras with $D = F$: 1 are still not

[6]) The importance of this can be understood from the following. As is known, a parabolic mirror can only be used for observing an infinitely remote object. If the object is at a finite distance then an elliptical mirror has to be used, with the object and the image in the two foci of the ellipsoid. When the distance of the object changes one therefore needs another elliptical mirror. The same applies to the Schmidt optical systems. When changing over from an infinitely remote object to one at a finite distance the correction plate has to be made "stronger". The required strength of the correction plate depends upon the distance of the object.

[7]) G. Z. Dimitroff and J. G. Baker, Telescopes and accessories, Blakiston Company, Philadelphia 1946, p. 292.

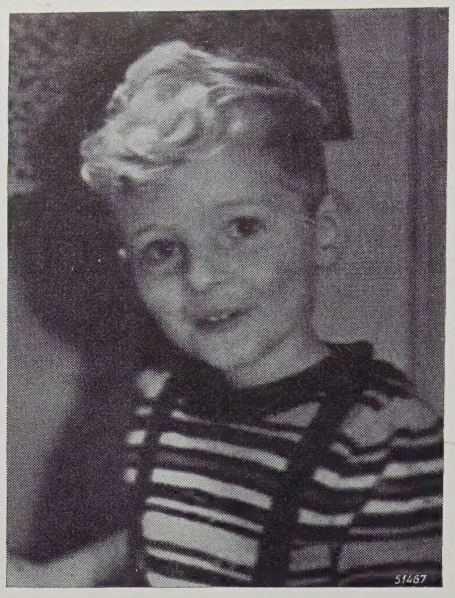

Fig. 8. Photograph taken with a camera made in the Philips laboratory at Eindhoven with a Schmidt optical system and a gelatin correction plate ($D = F : 0.7$). This optical system is of such a high power that the photo could be taken without any other illumination than that from a 25 W lamp and an exposure time of 1/10 sec.

the most rapid, some having been built even with $D = F : 0.6$.

The fact that good photographs of the constellations can be taken with the Schmidt optical system and simple accessories is demonstrated by *fig. 7*, where a photograph is reproduced, taken in the Philips laboratory at Eindhoven, of a part of the Orion constellation. A Schmidt mirror system with a focal distance of 8 cm was used. Although the field of vision has a diameter of no less than 20° the image is sharp and free of aberrations right up to the edges of the photograph.

The possibilities of application of the Schmidt optical systems is not confined to astronomy. This sytem has been applied in our laboratory in the construction of cameras of high optical power for experimental use (see *fig. 8*). Two other applications have already been mentioned in passing: cameras for photographing X-ray images on a fluorescent screen, and projectors as used in television receivers. It is the intention to describe the Schmidt optical systems designed for these purposes in a subsequent issue of this journal in due course.

CIRCUIT FOR CONDENSER MICROPHONES WITH LOW NOISE LEVEL

by J. J. ZAALBERG van ZELST. 621.395.616:621.395.822

Hitherto the condenser-microphone has generally been used in series with a direct voltage source and a resistor. The resistance of the latter must be of a high value, not only to obtain good reproduction of the low notes but also in view of the noise level. This high value of the resistance, however, makes it necessary to build in an amplifying valve close to the microphone. The same is also necessary with another method where the microphone forms part of the high-frequency oscillating circuit of an oscillator. There is a third method, dealt with more extensively here, which does not have this drawback and, moreover, is characterized by an exceptionally low noise level. With this method the microphone is incorporated in a bridge circuit which, as the diaphragm vibrates, supplies an amplitude-modulated high-frequency voltage. This voltage is amplified and detected. The bridge circuit (including the microphone but without valve) can be connected to the amplifier by means of a cable. This method is equally suitable for other capacitive vibration pick-ups, e.g. a capacitive gramophone pick-up.

The condenser-microphone working on direct voltage

In the previous issue of this journal [1]) a type of condenser-microphone was described which excels by its uniform reproduction of the audio frequencies and at the same time has a high degree of sensitivity and is of small dimensions. However, when used in what might be called the "conventional" circuit this new design still has some drawbacks in common with the older types of condenser-microphones. In this circuit (*fig. 1*) the microphone works on direct voltage and is in series with a resistor R. This resistor is given a high value for two reasons:

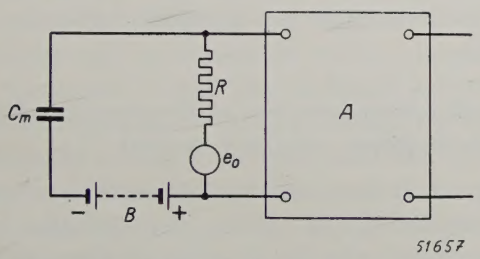

Fig. 1. Conventional circuit of a condenser-microphone (C_m). B is a source of direct voltage, R a resistor of high impedance, A an amplifier; e_o represents the noise voltage coming from R.

1) As explained in the article referred to [1]), for the sake of good reproduction of the low notes the charge of the condenser formed by the microphone must remain practically constant when the diaphragm vibrates. The condition required for this is that $2\pi f C_m R$ must be at least of the order of unity (C_m = capacitance of the microphone), also for the lowest frequency $f = f_1$, which has to be reproduced well. With $f_1 = 30$ c/s and $C_m = 50$ pF this means that the resistance R must be of the order of 100 megohms.

2) The second reason why R has to have a high value is connected with the noise, the source of which lies in this resistor.

The average value $\overline{e}$ of the quadratic contribution to the noise voltage, in a frequency band Δf, amounts to [2]):

$$\overline{e_0^2} = 4\,kTR \cdot \Delta f, \quad . \quad . \quad . \quad . \quad . \quad (1)$$

in which k represents Boltzmann's constant ($1.38 \cdot 10^{-23}$ Wsec/degree) and T the absolute temperature of the resistor. In the case of the condenser-microphone, in an equivalent circuit one can imagine that noise-voltage source as being connected in series with the resistor and the microphone (fig. 1). What has to be considered is that part of this noise voltage which occurs across the input terminals of the amplifier, thus also across the capacitance C_m. The average quadratic contribution $\overline{e^2}$ to the noise voltage across C_m, in a frequency band Δf, is calculated from (1):

$$\overline{e^2} = 4\,kT \cdot \frac{R}{1 + (2\pi f\, C_m\, R)^2} \cdot \Delta f. \quad . \quad . \quad . \quad (2)$$

The total contribution in a frequency range extending from f_1 to f_2 is found by integrating (2) between the limits f_1 and f_2; thus, for the range of the audible notes, from f_1 = about 30 c/s to f_2 = about 14 000 c/s. For values of R greater than $R_{\min} = 1/(2\pi f_1 C_m)$ (i.e. approximately the minimum required for good reproduction of the low notes) the rule holds that in each frequency interval Δf lying above f_1 the contribution to the noise becomes smaller as R increases. This may be seen in *fig. 2*, where the fraction $R/[1 + (2\pi f C_m R)^2]$ occurring in

[1]) A. Rademakers, A condenser-microphone for stereophony, Philips Techn. Rev. **9**, 330-338. 1947 (No. 11).

[2]) See *e.g.* Philips Techn. Rev. **2**, 140, 1937 or **6**, 130, 1941.

(2) is plotted as a function of f for one value of C_m and two values of R: curve (1) for $R = R_{min}$, (2) for $R = 2R_{min}$. To the right of f_1 curve (2) lies entirely underneath (1). A lower noise level is therefore obtained by choosing R greater than R_{min}.

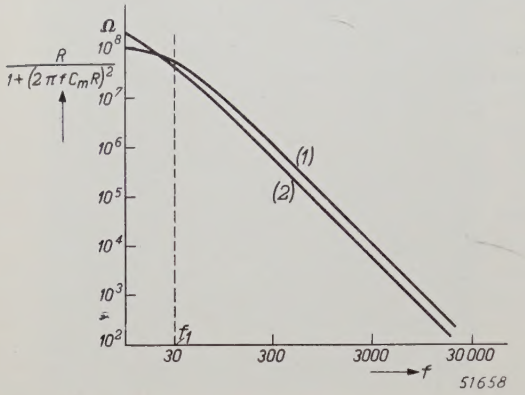

Fig. 2. The factor $R/[1 + (2\pi f C_m R)^2]$, represented here as a function of the frequency f in c/s, in the diagram of fig. 1 is a measure for the contribution to the noise (in a frequency interval Δf) at the input of the amplifier. Curve (1) applies for the smallest value of R which with a given value of C_m yields a satisfactory reproduction of the lowest frequency f_1; curve (2) applies for twice as high a value of R. Curve (2) lies below curve (1) to the right of f_1. This diagram applies for $f_1 = 30$ c/s, $C_m = 50$ pF, $R = 100$ and 200 megohms.

The drawbacks mentioned above as being connected with the conventional circuit of the condenser-microphone are related to the high value of the resistance connected in series with the microphone. These drawbacks are the following:

a) The circuit in which the microphone is taken up is highly sensitive to low-frequency interference which may be induced in it, for instance by neighbouring a.c. mains.

b) The insulation of the microphone and of the grid of the first amplifying valve has to answer very high requirements.

c) The microphone cannot be connected directly to a cable, because the capacitance of the cable would then be in parallel with that of the microphone, so that variations in the cable capacitance — caused by bending, clinching, twisting, etc. of the cable — would induce interfering voltages. Consequently one is obliged to build in an amplifying valve, with accessories, near the microphone. In many cases this means an awkward complication.

The first-mentioned difficulty can be overcome by providing adequate screening. The second one can be partly met by employing a low series resistance; in order still to satisfy the requirement of $2\pi f_1 C_m R > 1$ it is necessary to increase C_m proportionately, by connecting a fixed condenser in parallel to the microphone. In the article referred to in footnote [1]) it was stated, for instance, that R had been reduced from 80 to 5 megohms and C_m raised from 65 to 1000 pF. This, however, still does not overcome the necessity of having to build in an amplifier near the microphone. Moreover, yet another difficulty has to be taken into the bargain:

d) Both the absolute sensitivity decreases (because the relative capacitance variations — and thus also the resultant voltage variations — become just as many times smaller as C_m is increased) and also the signal-to-noise ratio, because the noise voltage decreases only in proportion to $\sqrt{C_m}$.

All these difficulties are, as already stated, a direct result of the fact that the microphone is connected in series with a high resistance, such being unavoidable when working on direct voltage, and one does not wish to sacrifice anything in quality. For a long time already other circuits have been known which dispense with the high resistance. With such circuits a high-frequency alternating current flows through the microphone, whilst the high-frequency voltage on the microphone is modulated in some way or other by the speech oscillations. The high-frequency current is to be regarded as an auxiliary current with which the impedance of the microphone, varying at low frequencies, is "measured" or "scanned" as it were.

We shall consider two methods based on this principle.

The condenser-microphone as frequency-modulator of a high-frequency auxiliary current

Riegger [3]) has indicated a method where a condenser-microphone forms part of the high-frequency oscillation circuit of an oscillator, so that certain frequency changes correspond to the variations in capacitance. By means of suitable circuits an amplitude-modulated signal is obtained which corresponds to this frequency modulation and which after detection produces a low-frequency signal.

When this method was published in 1924 it did not meet with much success, partly because of the then inadequate means of detecting frequency-modulated signals. Since there are now better means available, Riegger's method could be applied more successfully, that is to say a fairly high sensitivity, a reasonably low noise level and little trouble from low-frequency induction interferences may be expected. It still has the drawback, however, that a valve — the oscillator valve — with accessories

[3]) Z. techn. Phys. **5**, 579. 1924.

has to be built in near the microphone. Moreover, it is rather complicated and highly sensitive to variations in the values of various circuit elements.

The condenser-microphone as amplitude modulator of a high-frequency auxiliary current

We shall go somewhat more closely into another method with high-frequency supply which has none of the abovementioned drawbacks attaching to it. According to this method a constant current I is sent through the microphone with a likewise constant high frequency (the carrier-wave frequency, $= \omega_0/2\pi$). The voltage on the microphone is proportional to $1/C_m$ and thus varies in amplitude when the capacitance C_m changes in consequence of the sound vibrations.

The relative variations in capacitance, however, are as a rule very small; in this manner one would then get only a small modulation depth. As a consequence the signal would bear an unsatisfactory relation to the noise, which now is not due to a resistor (for there is no resistor here) but partly to fluctuations in the amplitude of the high-frequency supply current and partly to fluctations of the carrier-wave frequency. The current drawn from an oscillator is unavoidably modulated with noise both in amplitude and in frequency. When the current modulated in frequency with noise flows through an impedance which is dependent on the frequency — and the condenser microphone is such an impedance — then a voltage arises which is modulated in amplitude with noise and which combines with the noise voltage coming directly from the amplitude-noise of the supply current.

Furthermore, there is still the abovementioned difficulty that when the microphone is connected to a cable the variations in capacitance of that cable make themselves felt as interferences.

From what follows it will be seen, however, that all these difficulties can be removed.

Tuning of the microphone circuit

The first improvement to be made is to connect the microphone in series with a coil — for the present assumed to be free of loss — the self-inductance of which at the carrier-wave frequency is approximately in resonance with the microphone capacitance. The addition of the constant impedance of this coil does not affect the size of the absolute impedance variations occurring in the circuit when the diaphragm vibrates, but it affects the total impedance, which becomes very small. Thus the relative impedance variations increase considerably, and consequently so does the modulation depth.

Thanks to the fact that the impedance formed by the coil of the microphone in series is so low, the noise components of the current will not induce any noise voltage worth mentioning. At the same time another impedance — a cable — can be connected in parallel to this low impedance without any objection, so that the microphone can then indeed be connected direct to a cable (*fig. 3*). There is still the drawback, however, that the impedance is frequency-dependent; frequency fluctuations will therefore still give rise to noise.

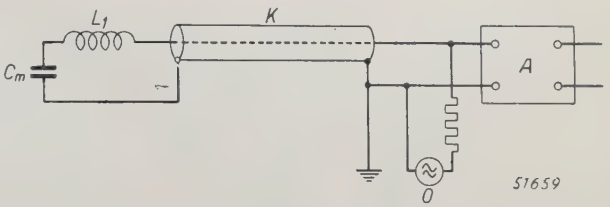

Fig. 3. The oscillator O sends a constant current with a constant frequency through the condenser microphone C_m and the coil L_1, which are tuned approximately to the frequency of the oscillator. Vibrations of the microphone diaphragm set up variations in capacitance, as a consequence of which the high-frequency voltage on the microphone is modulated in amplitude according to the sound vibrations. Owing to the low impedance of L_1-C_m the connection to the microphone can safely be made by means of a cable K. A is the amplifier, serving at the same time as detector.

Finally it has to be considered that the coil will actually have a certain loss resistance r. In the first place this resistance forms a source of noise — though it may be a feeble one — but it involves yet another difficulty of a different nature. Contrary to what would be the case with a loss-free coil, the output voltage has a carrier-wave component Ir shifted 90° in phase with respect to the original carrier-wave component. This would lead to distortion in the detection, to which we shall revert presently.

Bridge circuit

In order to circumvent also these difficulties we must extend our circuit somewhat. Instead of "measuring" the impedance of the series connection of microphone and coil direct, we compare it with that of a second branch consisting of an identical coil in series with a fixed condenser, the capacitance of which is just as large as that of the microphone in the state of rest (*fig. 4*). Equal currents are passed through the two branches, which together form a bridge; the difference V of the voltages arising on the branches serves as output voltage.

In the state of rest apparently $V = 0$, even

though the coils are not free of loss. When sound strikes the microphone then V consists only of side-band components. The carrier-wave component is absent and therefore has to be added in the detector stage; we shall see presently how this can be done.

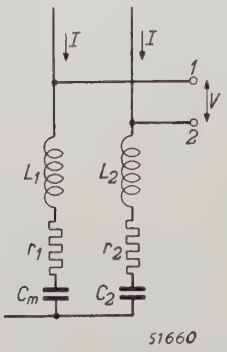

Fig. 4. Bridge circuit consisting of two branches L_1-r_1-C_m and L_2-r_2-C_2 with a high-frequency current I flowing through both. The self-inductances L_1 and L_2 are equal, as are also the loss resistances r_1 and r_2. The capacitance C_2 is equal to the microphone capacitance C_m when the diaphragm is at rest. The voltage V between the terminals *1* and *2* has no carrier-wave component, but consists of side bands corresponding to the sound striking the microphone.

How do matters stand now with the previously mentioned causes of noise which still remained, viz. the amplitude and frequency modulation of the current I with noise, and the loss resistance of the coils?

The two causes of noise occurring in the current I are now in principle rendered harmless, for with the diaphragm in the state of rest the bridge is in equilibrium for all frequencies, so that no noise voltage arising from the amplitude modulation of I occurs across the output terminals. And as regards the frequency modulation of I with noise, this too does not give rise to any voltage across the output when the diaphragm is in the state of rest, since the equal impedances of the bridge branches vary with the frequency in exactly the same way. When the equilibrium of the diaphragm is disturbed — owing to sound striking it — then the two noise components do indeed occur, but they do so in proportion to the relative variation in capacitance $(C_m—C_2)/C_2$, thus also proportionate to the sound pressure on the microphone.

Thus there remain as the only permanent source of noise the loss resistances of the coils. Actually we should add the mechanical vibration of the circuit elements and the wiring; this is accompanied by variations in capacitance or self-inductance, which may again constitute a source of noise.

Under this last heading are also the vibrations of the diaphragm when there is no "external" noise. A condenser microphone may also act as a telephone; there will thus be movement in the diaphragm when a noise-modulated current flows through the microphone. This is not the case with its opposite member in the bridge circuit — the condenser C_2 — so that the bridge is not in equilibrium and thus produces noise voltage. This effect, however, is found to be very small in comparison with the other noise effects.

Fig. 5 shows how the two branches can be fed from one oscillator with the introduction of a pentode in between. In the anode circuit of this pentode is an oscillating circuit with self-inductance L_a and a capacitance formed by the sum of the capacitances C_3 and C_4; the branches L_1-C_m and L_2-C_2 are each tuned to the oscillator frequency (and may therefore be regarded as short-circuits), as is also the circuit L_a-$(C_3 + C_4)$. The currents I (*fig. 4*) flowing through the two branches may amount, for instance, to 20-50 mA. The pentode need only yield a power of the order of 0.1 W, thanks to the impedance of the branches being so low. A small valve therefore suffices. If necessary a separate oscillator as indicated in fig. 5 can be dispensed with by causing the pentode itself to oscillate with the connected circuits.

It is now desirable to mention some numerical data. With sounds of a moderate strength the sound pressure (R.M.S. value of the alternating pressure) amounts to about 1 μbar. In the case of the microphone described in the article quoted in footnote [1]), this corresponds to a relative capacity change of about 1 : 30 000. The voltage V of the side

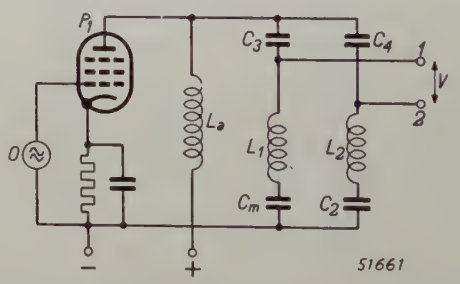

Fig. 5. System for feeding the two bridge branches (L_1-C_m and L_2-C_2) of fig. 4. O is an oscillator with the carrier-wave frequency, P_1 an amplifying valve (pentode), C_3 and C_4 are condensers in series with the two branches, L_a is a coil in resistance with $C_3 + C_4$, *1* and *2* are the terminals across which the modulated voltage arises.

bands (fig. 5) will then be about 1/30 000 of the voltage on the microphone. Owing to the danger of sparking between the electrodes this latter voltage is limited to 100 V. Consequently with a sound pressure of 1 μbar V will be about 3 mV.

What is the level of the noise voltage between

the terminals *1* and *2* (fig. 5)? This noise voltage will come mainly from the resistance between these terminals, thus from the resistance of the two coils together. A coil of good quality and having the required self-inductance has a resistance $r =$ approx. 15 Ohms. In the frequency range Δf from 0 to 14 000 c/s the noise voltage is then equal to

vibration of the wiring as a result of mechanical disturbances in the surroundings; in this particular case no special precautions had been taken. It was also found necessary to use components of very good quality, *i.e.* components not subject to fluctuations in their values.

Further, it is to be remarked that the system

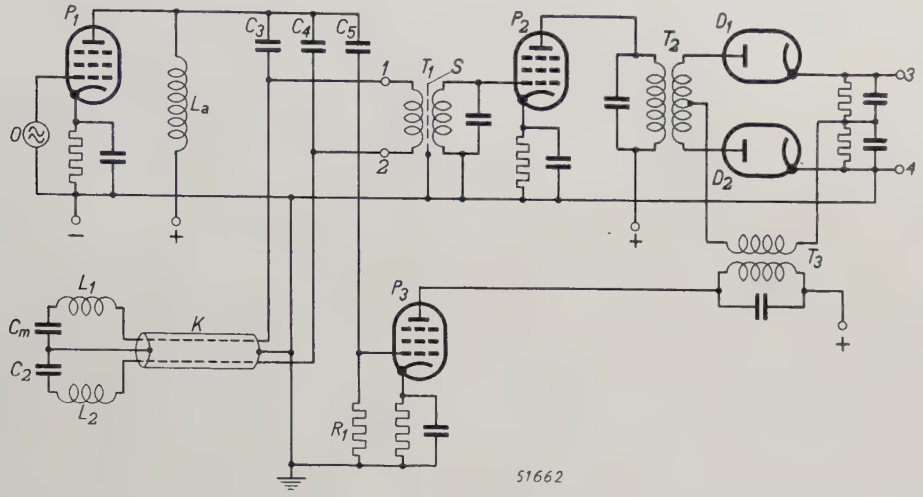

Fig. 6. Amplification and detection of a voltage between the terminals *1* and *2* (the part of the circuit to the left of these points corresponds to fig. 5). *K* is the microphone cable, T_1, T_2 and T_3 are transformers tuned to the carrier-wave frequency, P_2 and P_3 pentodes, D_1 and D_2 diodes for the detection. C_5 and R_1 form a phase-changing voltage divider. *3* and *4* are the output terminals for the low-frequency signal. Thanks to the diodes being in push-pull, no noise voltage from the carrier-wave channel (C_5-R_1-P_3-T_3) occurs on the output terminals. S = screen in T_1.

$\sqrt{4kT \cdot 2r \cdot \Delta f} = \sqrt{4 \cdot 1.38 \cdot 10^{-23} \cdot 300 \cdot 2 \cdot 15 \cdot 14\,000} = 8.4 \cdot 10^{-8}$ V $= 8.4 \cdot 10^{-5}$ mV. For an equally large signal voltage a sound pressure of $8.4 \cdot 10^{-5}/3 = 2.8 \cdot 10^{-5}$ μbar would be necessary, *i.e.* 17 db below the international zero level (10^{-16} W/cm²)! This is indeed exceptionally low. In order to maintain a very low noise level when amplifying and detecting (see the next sub-heading) care has to be taken to ensure that no appreciable amount of noise is added. For certain reasons, however, it may be desirable not to aim at the lowest possible noise level. One has to take into account, for instance, the characteristic impedance of the cable, which has to be approximately equal to the resistance of the coils. In one practical example the only cable available had a characteristic impedance of 160 Ohms, so that the resistance of the coils had to be increased to that value. With a further 80-Ohms resistance of a transformer at the end of the cable, in that case the noise resistance was $2 \times 160 + 80 = 400$ Ohms, corresponding to a noise level of —6 db. Direct measurement showed the actual noise to be a few db stronger. This has to be ascribed to the variation of stray capacitances due to the is much less sensitive for gradual variations in the values of the circuit elements than is the Riegger method.

Amplification and detection

The signal voltage V (fig. 5) is stepped up by a high-frequency transformer T_1 with a tuned secondary winding (*fig. 6*). Any low-frequency interferences that may be induced are short-circuited by the primary of T_1. The secondary voltage is amplified and detected.

Since the signal V does not primarily contain any component with the carrier-wave frequency, such a component has to be added in the detection stage. This is done by means of a separate carrier-wave channel consisting of the components C_5-R_1-P_3-T_3 (see fig. 6).

Care has to be taken that no noise is added from this carrier-wave channel and, moreover, that the carrier-wave voltage has the right phase. As to the first point, this has been provided for by arranging for the detection to take place in a push-pull circuit with two diodes; if symmetry is ensured then any noise present in the secondary voltage

from T_3 cannot reach the output terminals *3* and *4*.

The question of the right phase of the carrier-wave voltage is illustrated in *fig. 7*: fig. 7*a* represents the correct position, the carrier-wave voltage V_0 being in phase with the resultant V_r of the two side band components V_1 and V_2, so that the result is a carrier-wave voltage purely modulated in amplitude. In fig. 7*b* it is assumed that V_0 is shifted 90° with respect to V_r. During one cycle of the modulation frequency the vector sum of V_0 and V_r then varies considerably in phase but little in amplitude. The angular velocity of this vector is therefore no longer uniform; in other words, there is considerable frequency modulation. Moreover, the amplitude modulation takes place at a frequency twice that of the sound frequency. In the case of a different phase shift between V_0 and V_r we have an intermediate state where again amplitude and frequency modulation occur simultaneously. This is highly undesirable, because it leads to great distortion in the detection. Care must be taken therefore that the situation represented in fig. 7*a* is actually obtained.

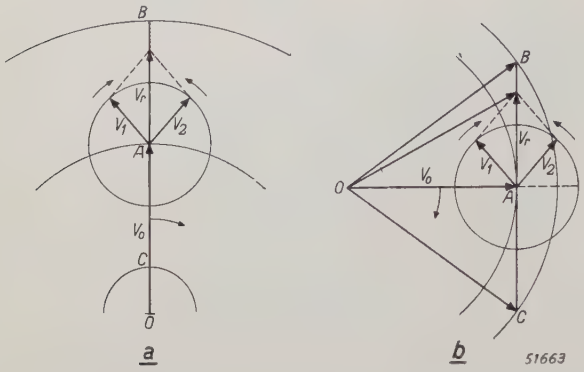

Fig. 7. The vector $OA = V_0$ represents the non-modulated carrier-wave; it rotates at an angular velocity corresponding to the carrier-wave frequency. The side bands are represented by the vectors V_1 and V_2, which turn about A in opposite directions at an angular velocity corresponding to the signal frequency. The resultant of V_1 and V_2 is V_r, a vector whose maximum size is equal to AB or AC. In fig. 7*a* V_0 has the right position with respect to V_r. The sum of V_0 and V_r is a vector which rotates with the same constant angular velocity as V_0 and which varies in amplitude between OB and OC. The result is pure amplitude modulation. In fig. 7*b* V_0 is turned with respect to V_r (in this case 90°). The vector sum of V_0 and V_r shows no constant angular velocity and varies only little in amplitude (from OA to $OB = OC$). This means that mainly frequency modulation occurs and amplitude modulation only to a small extent. In a detection system arranged for amplitude modulation this would lead to a distorted low-frequency signal.

To this end it must be borne in mind that the output voltage from the secondary tuned transformer T_1 (fig. 6) is shifted 90° with respect to the primary voltage. Consequently it is necessary to provide for an equally large phase shift between the input and output voltages of the carrier-wave channel. This is done with the aid of the voltage so that the voltage on R_1 is shifted almost 90° with divider C_5-R_1, which is so designed that $R_1 \ll 1/\omega_0 C_5$, respect to the anode alternating voltage of the tube P_1.

An earthed screen between the coils of T_1 prevents capacitive transmission to the secondary coil of the voltage with the carrier-wave frequency present between the points *1-2* and earth.

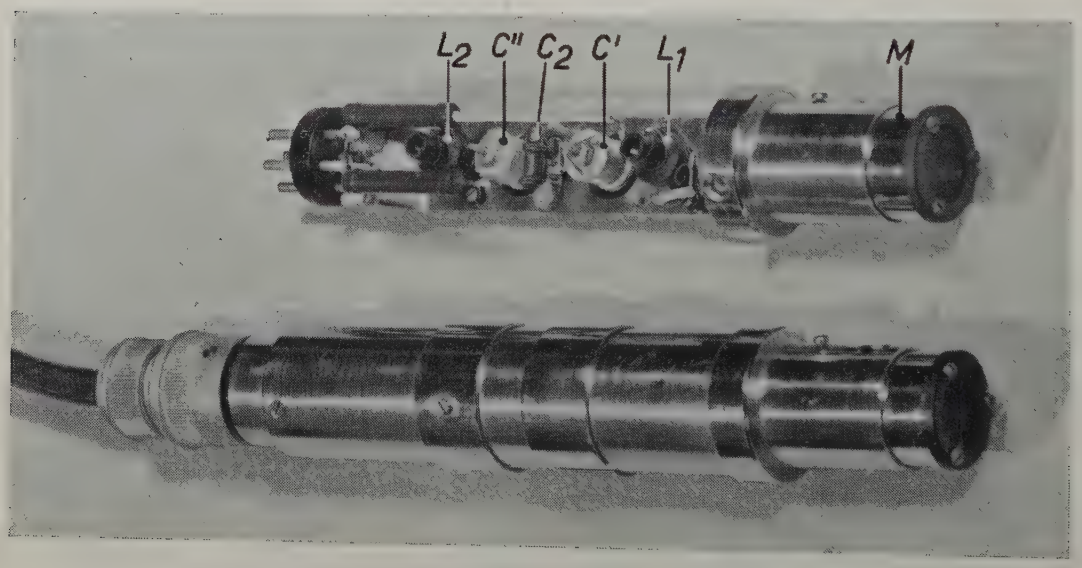

Fig. 8. Top: Opened condenser-microphone showing the component parts built in. M is the microphone proper; L_1, L_2 and C_2 have the same meaning as in fig. 6; the small adjusting condensers (trimmers) C' and C'' are connected in parallel to the microphone and to C_2 respectively. Bottom: The microphone encased and connected to a cable.

Fig. 8 shows a complete microphone connected to a cable and also a deceased microphone showing the components represented in the bottom left-hand corner of fig. 6.

It is to be added that the principle of the circuit described here is not new and is in fact even older than Riegger's system [4]). The great advantages it offers — low noise level and absence of an amplifier built in close to the microphone — have apparently not been realized hitherto and the methods had become more or less forgotten.

Other applications

In conclusion we would add that the method described here lends itself equally well for use in combination with a capacitive gramophone pick-up or any other capacitive pick-up for mechanical vibrations [5]). In principle it is also possible to modify the method for variable inductances instead of variable capacitances, thus, for instance, for electromagnetic vibration pick-ups (including microphones) reacting to the changes in self-inductance of a coil placed near to a vibrating iron membrane or armature.

[4]) See *e.g.* Swiss Patent 95 439 in the name of H. Vogt, J. Engl and J. Massolle.

[5]) P. J. Hagendoorn and M. F. Reynst, An electrical pressure indicator for internal combustion engines, Philips Techn. Rev. **5**, 348-356, 1940, especially fig. 3.

THE BLURRING OF X-RAY IMAGES

by H. A. KLASENS *)

537.531:778.33.022.8

Fluorescent screens cause blurring of the X-ray images. Here the factors governing this screen blurring are investigated. It is of importance that the magnitude of these factors should be expressed in the same terms as that of the geometrical and kinetic blurring. A method is described by means of which screen blurring is compared with kinetic blurring. It appears that the *S*-shaped curve which represents the distribution of intensity in the image of a sharp edge when using a fluorescent screen can be sufficiently characterized for this purpose by a straight line intersecting the *S*-curve at two points at a certain height. This method is applied for determining the screen blurring of a number of intensifying screens and viewing screens. It is also employed to find a formula for the total blurring when various kinds of blurring are combined.

In radiology fluorescent screens are used both for making the X-rays visible and for intensifying their photographic action. In an article published in the preceding number of this journal [1]) this conversion of X-ray energy into light energy was studied and the conditions with which X-ray screens have to comply in their various applications were discussed.

A drawback attaching to the employment of fluorescent screens is that they cause additional blurring of the image. In this article the cause of this screen blurring will be discussed and a method of expressing the magnitude of the effect numerically will be investigated. Further, we shall consider how its effect can be compared and combined with that of two other kinds of blurring, namely geometrical and kinetic blurring.

The cause of screen blurring

Fig. 1 gives a magnified representation of the cross section of part of an X-ray screen, in this case an intensifying screen. The fluorescent layer lies between a sheet of cardboard and the sensitized film. The arrows indicate the direction of the incident rays. This illustration applies to the case where the fluorescent layer is used as front screen; it may also be used as back screen, behind the film (as indicated in the article quoted in footnote [1])), which case will be considered farther on.

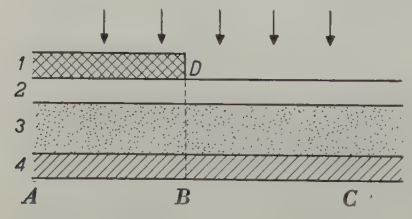

Fig. 1. Magnified cross section of a part of an X-ray screen (intensifying screen) with a lead plate having a sharp edge *D* laid upon it. *1* is the lead plate, *2* the cardboard base of the fluorescent layer, *3* and *4* the film. The arrows indicate the direction of the incident X-rays.

It is assumed that the screen is partly covered with a sheet of lead of such a thickness as to be practically impermeable for X-rays. We shall now consider what image the edge of the sheet of lead leaves on the film.

The image of the edge will be perfectly sharp when no light falls on the film to the left of *B*. Owing to the finite thickness of the fluorescent layer, however, this is not the case. The crystals in the part of this layer to the right of *BD* are brought to fluorescence by the X-rays. This light spreads out in both directions and consequently cannot be prevented from reaching that part of the film to the left of the line *BD*.

When we measure the distribution of light along the line *AC* we obtain a curve as represented in *fig. 2*. The two curves, (*a*) relating to an intensifying screen and (*b*) relating to a viewing screen, are symmetrical with respect to the point *M*, corresponding to point *B* in fig. 1.

The fact that the light distribution curves are symmetrical with respect to *M* can be readily understood from the following. We imagine the screen as extending over a large distance to the left and right of the line *BD*. The point *B* then receives light only from that part of the screen to the right of *BD* and the luminous intensity at that point is thus half of what it would be if the sheet of lead were removed. Let us now consider the points *A* and *C* at equal distances to the left and right of *B*. In addition to the light rays from the right, *C* receives light from the part above *BC*. The amount that *A* receives is less than that falling on *B*, by just this quantity, viz. the light that would be generated in the part above *AB* if the sheet of lead were removed.

*) Material Research Laboratory, Philips Electrical Ltd. London, England.

1) H. A. Klasens and W. de Groot, Light emission of X-ray screens, Philips Techn. Rev. **9**, 321-329, 1947 (No. 11).

The luminous intensity at A is therefore just as much below the value at B as the intensity at C is above it.

In order to observe more closely the spread of the light generated in the fluorescent screen, let us imagine that the sheet of lead is removed and also the whole of the screen except for one single crystal at a distance a from the film (*fig. 3*).

When irradiated with X-rays this crystal will emit a light flux which we shall call Φ. This causes an illumination at a point on the film of intensity

$$E = \frac{a\Phi}{4\pi (r^2 + a^2)^{3/2}},$$

where r is the distance from the base of a perpendicular drawn from the crystal on the film to the point in question.

The curves in fig. 3 represent the variation in luminous intensity for two values of a. The larger the value of a, the flatter are the curves. The luminous crystal produces on the film a spot of light which becomes more diffused as the crystal is farther removed from the film.

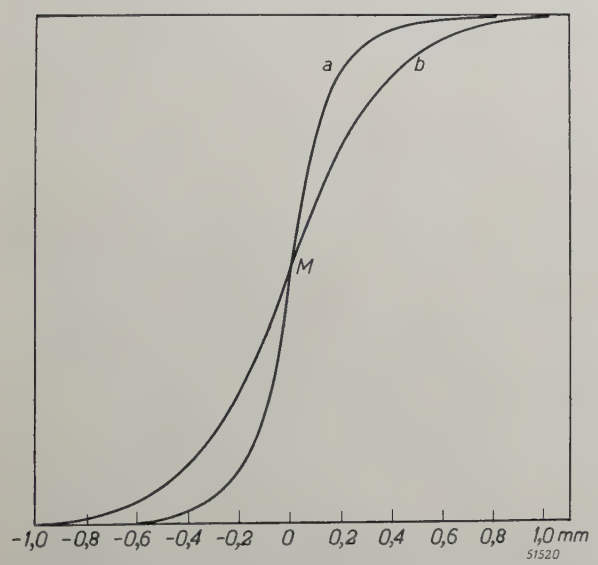

Fig. 2. The luminous intensity curve in the image of the edge of a metal plate on a film obtained with the aid of a fluorescent screen; *a*) when using an intensifying screen of fine-grained calcium tungstate; *b*) with a viewing screen of coarse-grained zinc-cadmium-sulphide. Both curves are symmetrical with respect to point M, corresponding to point B in fig. 1.

When a light-absorbing medium is placed between the fluorescent crystal and the film we have a luminous intensity

$$E = \frac{a\Phi}{4\pi (r^2 + a^2)^{3/2}} e^{-\tau(r^2+a^2)^{1/2}},$$

where τ represents the absorption coefficient of the medium. The full curves then change into the dotted ones. It can be seen that not only does the luminous intensity decrease more strongly with increasing distance between the crystal and the film but also that the light does not spread out so far.

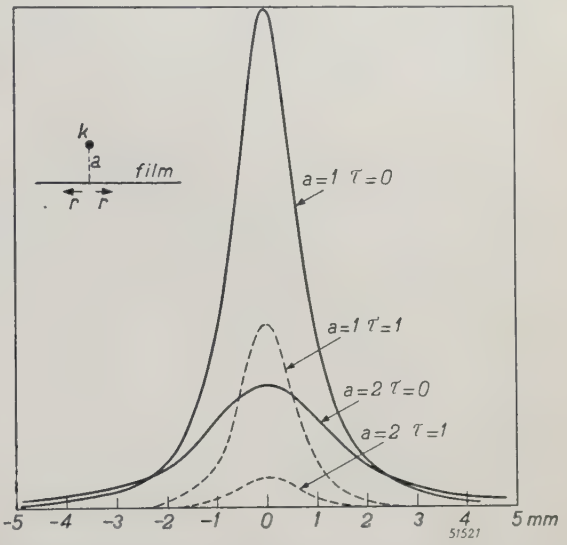

Fig. 3. Distribution of the luminous intensity on the screen resulting from the irradiation of a single crystal at a distance of a cm from the film. The full curves relate to the cases where a is 1 and 2 cm respectively and the absorption coefficient $\tau = 0$. The dotted curves apply to the cases where a is 1 and 2 cm and $\tau = 1$. In the inset k represents the crystal and r the distance from the point of the film in question to the base of the perpendicular drawn from k onto the film.

If we concentrate upon the spreading of the light from one crystal then, to a first approximation, we may regard the action of the rest of the screen as being that of an absorbent medium. Actually, however, the light is not only absorbed but also repeatedly reflected (scattered). The result is, on the one hand, that the actual length of the path travelled by the rays of light in the fluorescent layer is lengthened by repeated reflection, thereby intensifying the action of absorption; on the other hand however other crystals adjacent to the one originally considered act as if they were new sources of light, thus resulting in expansion of the spot of light. The question which of these two influences predominates is not easily decided and, as far as we know, has not been sufficiently investigated theoretically. It has been established in practice that as a rule increased scattering has a favourable effect on the blurring.

The blurring of the image as expressed in the curves of fig. 2 is caused by the spreading of the light of all the irradiated crystals together. Further expanding our theory for the single crystals, we arrive at the following conclusions:

1) The crystals in the screen farthest away from the film contribute most to the blurring. Thus the blurring diminishes the thinner the layer.
2) Blurring can be reduced by increasing absorption in the screen. This can be achieved by:
   a) increasing the actual absorption, for instance by adding a dyestuff to the binder,
   b) intensifying the scattering by using smaller crystals.

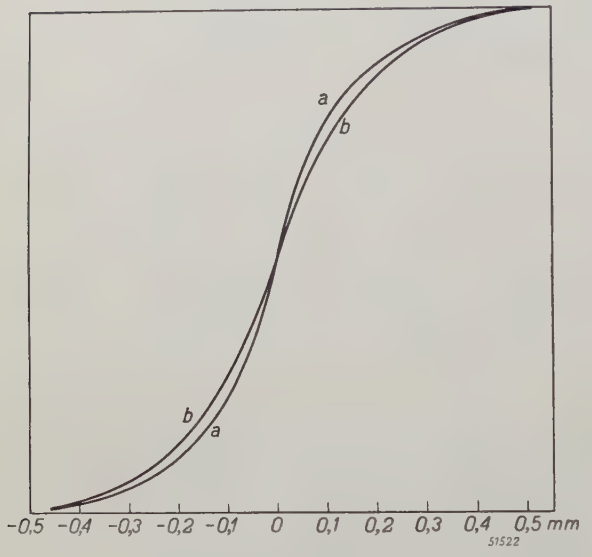

Fig. 4. The luminous intensity distribution in the image of a metal edge on a film obtained with an intensifying screen; *a*) when the screen is used as back screen, *b*) when the same screen is used as front screen. In the former case there is less screen blurring.

All these factors tending to reduce blurring have at the same time the effect of reducing the brightness of the screen, so that any gain in sharpness is always accompanied by a loss in brightness.

Screen blurring depends not only upon the nature of the screen but also upon the manner in which the light is generated in the screen. In the screen the intensity of the X-rays decreases exponentially. Consequently the greater part of the light is generated on that side of the fluorescent layer which is turned towards the X-ray tube. When the screen is used as back screen then that side is in contact with the film. Most of the light therefore comes from a layer which contributes least towards the blurring. When, however, the same screen is used as front screen the reverse is the case, most of the light then coming from a layer farther removed from the film. *Fig. 4* illustrates how this difference affects the light distribution curve of an edge image.

Measuring screen blurring

Apart from screen blurring, in radiology we encounter geometrical and kinetic blurring [2]). It is therefore of importance to know what happens when all these kinds of blurring occur together. It is above all necessary to be able to express these three blurrings by one and the same measure.

Geometrical blurring is caused by the finite width of the focus. Let us consider again the image cast on a photographic film by an object with a sharp edge. The distribution of energy from the X-rays along a line perpendicular to the shadow of the edge of the object is represented in *fig. 5a*.

A similar energy distribution is also obtained when the object is in motion during the exposure if the geometrical blurring in the radiograph can be ignored, for instance by making the focus small or holding the object close to the film. This is shown in fig. 5*b*. Kinetic blurring is particularly important when photographing the lungs, the heart and the stomach of the human body.

In both cases the energy reaching the screen or the film increases linearly from the minimum value in the shadow corresponding to the irradiation passing through the object to the maximum value in the area freely exposed. It is obvious to define these blurrings by the distance or the transition

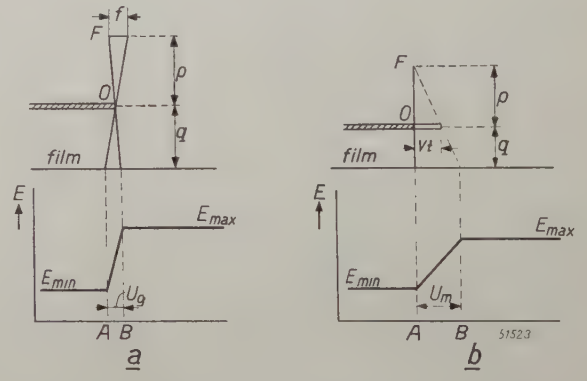

Fig. 5. *a*) Distribution of the energy E of the X-rays in the shadow of a stationary object O; f is the width of the focus F, $AB = u_g$ is the geometrical blurring.
b) Distribution of the X-ray energy in the shadow of a moving object. $AB = u_m$ is the kinetic blurring. Since the focus is considered as a point, in this case the geometrical blurring is zero.

from the minimum to the maximum energy (AB in fig. 5).

Given a focus width of f mm, a distance p from object to focus and a distance q from object to film,

[2]) These three kinds of blurring have already been discussed in previous articles in this journal. Cf. Philips Techn. Rev. **5**, 270-275, 1940; **8**, 32;-329, 1946 (No. 11).

the geometrical blurring is represented by

$$u_g = \frac{q}{p} \cdot f \quad \ldots\ldots\ldots \quad (1)$$

and the kinetic blurring by

$$u_m = \frac{p+q}{p} \cdot vt, \quad \ldots\ldots \quad (2)$$

in which v is the speed of motion in a direction perpendicular to the edge of the object and t the exposure time. The geometrical and kinetic blurring can therefore be deduced directly from the conditions under which the photograph is taken.

A clearly defined specification of screen blurring should conform to the same requirements. This is often overlooked. Screen blurring is frequently judged according to the clearness of details in the photograph, but there are many other factors playing a part, for instance the exposure time and the contrast. A photograph with a certain geometrical blurring may appear to be sharper when the contrast is intensified. A difference in the exposure time may entirely alter the character of an image. Spiegler has given some striking examples of this [3]). In order to avoid these difficulties any definition of screen blurring should be based solely upon the intensity distribution of the light in the screen image.

To arrive at such a definition it is best to start once more from the image of the edge of a plate. We then have to develop a method which makes it possible to arrive at a definition of screen blurring which is directly comparable with a blurring having a linear intensity variation.

Nemet, Cox and Walker [4]) have studied the blackening in an edge image on a film obtained with the aid of a fluorescent screen. The geometrical blurring was negligible and there was no kinetic blurring. From the blackening observed they deduced the luminous intensity distribution in the edge image on the screen. This was done while determining at the same time the blackening curve of the film, i.e. the curve indicating the relation between the blackening and the amount of light absorbed. The luminous intensity distribution E found on the screen was represented by an S-shaped curve (just as in the figs. 2 and 4) and this has been reproduced in *fig. 6*.

[3]) G. Spiegler, Photogr. J. **83**, 410-413, 1943.

[4]) A. Nemet, W. F. Cox and G. B. Walker, Brit. J. Radiology **19**, 257-271, 1946 (No. 223). The method followed by these investigators was developed on the basis of a method previously applied by Nitka, who, however, did not first convert the blackening curve into a luminious intensity curve; cf. H. Nitka Phys. Z. **39**, 436-439, 1938.

In order to arrive at a definition of the screen blurring these investigators measure the area of the shaded parts I and II in fig. 6. If we had to do with a geometrical or kinetic blurring u then the intensity distribution would not be represented by an S-shaped curve but by a straight line. If we indicate the area of $I + II$ by A then in that case the formula applying would be:

$$A = {}^1/_4 \, u \, (E_{max} - E_{min})$$

$$\text{or } u = \frac{4A}{E_{max} - E_{min}}, \quad \ldots\ldots\ldots \quad (3)$$

where E_{max} and E_{min} represent respectively the maximum and the minimum blackening.

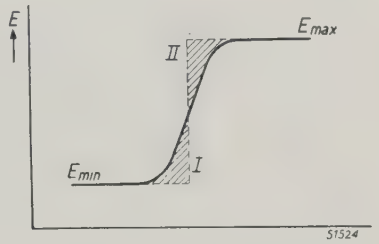

Fig. 6. The luminous intensity E in the image of an edge is distributed, owing to screen blurring, according to an S-shaped curve. Nemet, Cox and Walker take the sum A of the areas I and II for defining the screen blurring, putting $u_s = 4A/(E_{max} - E_{min})$, where E_{max} and E_{min} are respectively the maximum and the minimum luminous intensities in an edge image on a film.

Nemet, Cox and Walker now define the screen blurring u_s, in accordance with (3), by the equation:

$$u_s = \frac{4A}{E_{max} - E_{min}} \quad \ldots\ldots\ldots \quad (4)$$

This definition makes it possible to express the screen blurring in the same measure as the geometrical and kinetic blurring. It is not a priori certain, however, that screen blurring and geometrical or kinetic blurring, represented according to this method by the same number, will make the same impression upon the eye.

We have employed an experimental method for comparing screen blurring with kinetic blurring [5]), again using an edge image. The object used was a copper plate 0.2 mm thick, brought into contact with a casette containing the screen to be examined and a panchromatic film, in such a way that the edge of the copper plate was projected onto the middle of the film. The conditions of exposure (the voltage was 70 kV) were so chosen that the density on the film was about 0.4 in the shadow and 0.8

[5]) See also Philips Research Reports **1**, 241-249, 1946 (No. 4).

in the freely exposed part, it having been found that with the particular film used the blackening in that range varied practically linearly with the luminous intensity, so that the blackening curve indicated directly the variation of the luminous intensity.

Another piece of the same metal plate was mounted on an iron rod in the manner shown in *fig. 7*.

Fig. 7. Device employed to obtain a series of varied kinetic blurrings. a = iron rod, b = copper plate, c = hinge.

This rod was hinged at one end. Thus it was possible to move the plate during exposure over a distance varying from 0.3 mm at one end of the copper plate to 1.2 mm at the other end. No intensifying screen was used, so that there was no screen blurring. By holding the casette with the film close to the copper plate we obtained an image of the edge of the plate without any geometrical blurring and with a kinetic blurring which increased from 0.3 mm at one end to 1.2 mm at the other end. The conditions of exposure were so chosen that the image showed the same maximum and minimum blackening as that of the image which had only screen blurring.

The edge image with screen blurring and that with kinetic blurring were then compared with each other in a viewing lantern. Owing to the difference in the character of the two blurrings this comparison was rather difficult. For instance, when looking at a photograph with kinetic blurring under a very bright light one had the illusion of observing bright and dark lines parallel to the edge. In order to avoid this the brightness of the light in the viewing lantern had to be reduced to below the usual level.

The question to be decided was what parts of the image with kinetic blurring gave the same impression of blurring as the image with screen blurring. Ten observers were asked to give their impressions and from these an average was taken. This investigation was carried out with a blue intensifying screen and a yellow viewing screen, and it was found that the screen blurrings corresponded to kinetic blurring of 0.46 and 0.92 mm repectively.

The *S*-curve in *fig. 8* represents the energy distribution observed in the case of the edge image with a screen blurring of 0.92 mm. The straight line represents the energy distribution in an image with a kinetic blurring of 0.92 mm. A similar drawing has also been made for the screen and kinetic blurrings of 0.46 mm. The *S*-curve and the straight line intersect in both cases close to the points where $E = E_{min} + 0.16\ (E_{max}\text{-}E_{min})$ and $E = E_{min} + 0.84\ (E_{max}\text{-}E_{min})$.

This having been established, it is possible to determine the blurring of other screens by a much quicker method than that outlined above. First the energy distribution in an edge image is determined and plotted for any arbitrary screen. Then a straight line is drawn through the points where $E\text{-}E_{min} = 0.16\ (E_{max}\text{-}E_{min})$ and $0.84\ (E_{max}\text{-}E_{min})$. The distance between the points where according to this linear distribution the energy would be exactly equal to E_{max} and E_{min} (the points A and B in fig. 8) is then taken as a measure for the screen blurring.

We have applied this method to determine the blurring of a number of commonly used screens. In the case of combinations of intensifying screens (i.e. a front and a back screen) the results appeared to lie between 0.25 and 0.50 mm, and in the case of viewing screens between 0.4 and 1.0 mm.

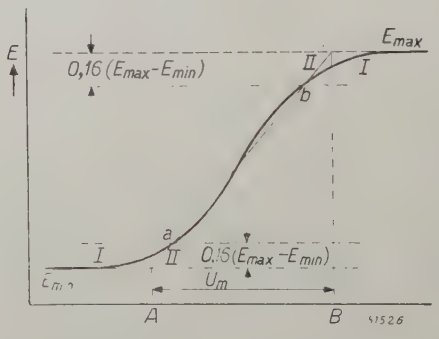

Fig. 8. The *S*-shaped curve *I* represents the energy distribution in an edge image with a screen blurring of the same magnitude as the kinetic blurring u_m to which the energy distribution according to the straight line *II* corresponds. The straight line passes through the points a and b for which $E—E_{min} = 0.16\ (E_{max}—E_{min})$ and $0.84\ (E_{max}—E_{min})$ respectively. The distance AB, which in this case is 0.92 mm, is a measure of the screen blurring.

Thus we have another method for deriving a measure for the blurring direct from the blackening or luminous intensity curve. This method, compared with that of Nemet, Cox and Walker, offers greater certainty of the adequacy of the measure, it having been established experimentally that two photographs having equal blurring according to the present definition, e.g. screen blurring and geometrical blurring, make the same impression upon the eye.

The Nemet, Cox and Walker method would have yielded slightly higher values for the blurring

of the screens referred to, but the difference is of no great importance.

Combination of screen blurring with other kinds of blurring

Screen blurring can easily be combined with geometrical and kinetic blurring by holding the copper plate a certain distance away from the casette containing the film and screen and moving it during exposure by means of the device shown in fig. 7. The total blurring then resulting can be measured by the method described. In this manner a formula can be deduced for determining the resulting blurring when various kinds of blurring are combined.

For screens with little blurring, such as those usually employed in normal contact photography, the blurring observed can well be represented by the formula

$$u = (u_g^3 + u_m^3 + u_s^3)^{1/3}, \quad . \quad . \quad . \quad . \quad (5)$$

where u_g is the geometrical blurring
u_m the kinetic blurring and
u_s the screen blurring.

The same formula applies also for a combination of geometrical and kinetic blurring ($u_s = 0$).

In the case of viewing screens with a blurring of the order of 0.7 mm the value observed is usually slightly higher than that obtained by calculation from equation (5), the average deviation being of the order of 5%. In practice such differences are scarcely noticeable.

We have also investigated whether the formula used by Newell [6]), viz.

$$u = (u_g^2 + u_m^2 + u_s^2)^{1/2} \quad . \quad . \quad . \quad . \quad (6)$$

properly represents what is actually observed. It appeared that the resulting blurring is always less than the square root of the sum of the squares of the component blurrings. The average deviation, however, is not greater than 10%. This means that the formula (6) likewise gives a reasonable approximation of the edge blurring, although the deviation is much greater than that of the formula (5).

---

[6]) R. R. Newell, Radiology **30**, 493-499, 1938.

THE MANUFACTURE OF PAPER CONDENSERS

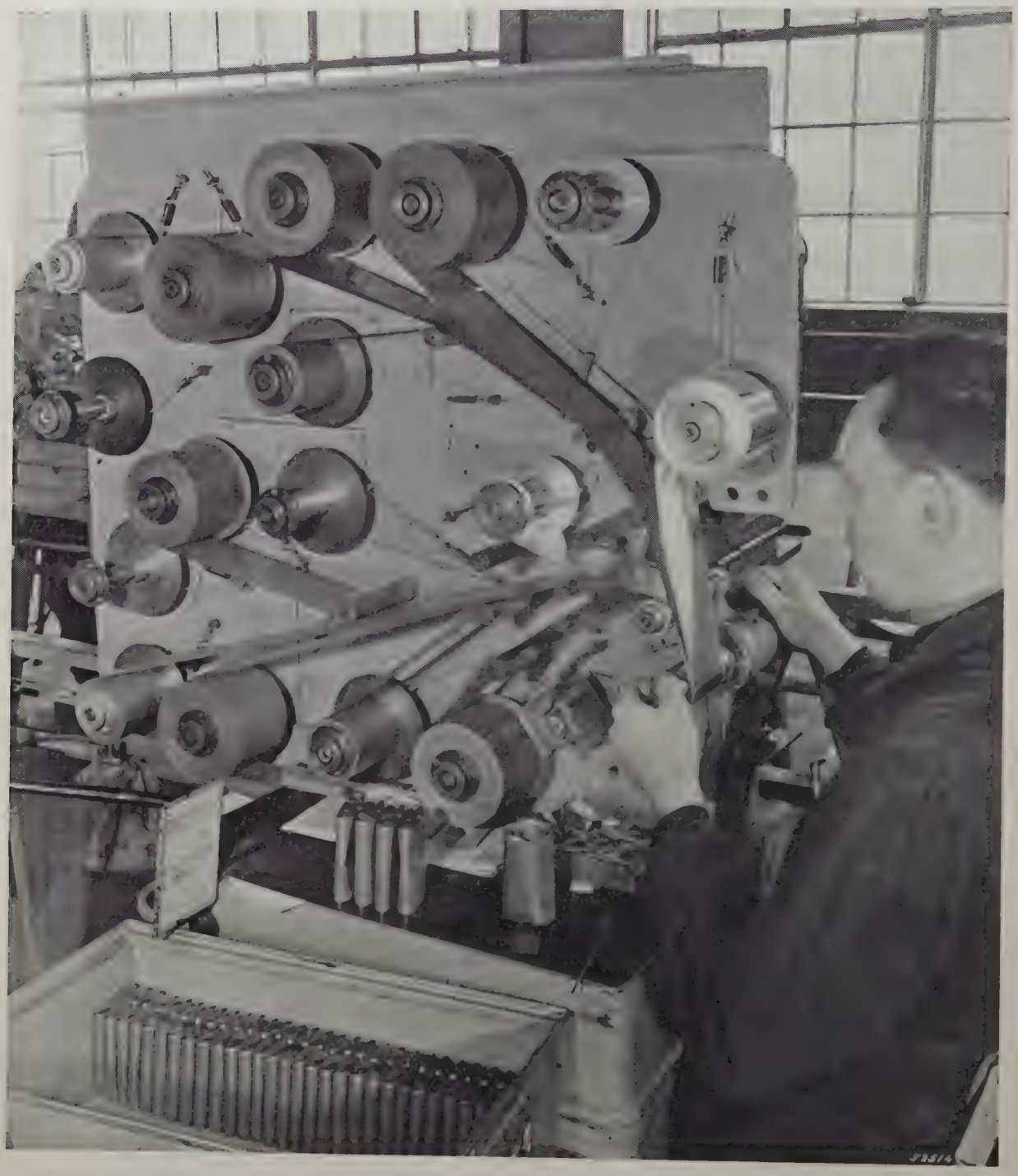

This photograph shows how paper condensers are wound. The outer covering of aluminium foil is fed from the two polished rollers. The dielectric consists of layers of paper, which are fed from the other rollers; the number of layers and the thickness of each depend upon the voltages for which the condensers are made. Here five layers are being wound. A second set of layers is required to prevent the coverings from making contact with each other. The circuiting contacts are made of strips of copper foil, seen underneath the left hand of the winder. When the counter (to the left of the man's left hand) shows the number of turns required for the particular capacity, the coil is taken off the pin and pressed flat, giving it the shape seen in the tray at the bottom. In the next stage the coils are provided with the electrical connections and placed in a metal box, which is then impregnated under vacuum and sealed by soldering.

MEASURING REVERBERATION TIME BY THE METHOD OF EXPONENTIALLY INCREASING AMPLIFICATION

by W. TAK

534.844.1:621.317.351:621.314.3

The reverberation time of an enclosed space can be measured by producing in that space periodical sound impulses and conducting the voltage from a microphone set up within the space to an oscillograph *via* an exponential amplifier. The amplification begins every time with a low value but increases exponentially with the time by a certain amount, say 60 db, and then drops back to the initial low value. The rhythm of the sound impulses and of the exponential variation in amplification is determined by the generator of the time-base voltage of the oscillograph. The frequency of this voltage is regulated in such a way that the oscillogram shows as far as possible a constant amplitude; when that is the case then the period corresponding to that frequency is approximately equal to the reverberation time sought. Various parts of the apparatus and some measuring results are described. At the same time it is demonstrated experimentally that when a sound is produced it excites mainly the characteristic vibrations of the space with the adjacent frequencies and that beats arise between those frequencies.

Introduction

The phenomenon of reverberation is of great importance when judging the acoustics of halls and rooms. The theory of this phenomenon and of the measuring of the reverberation time has been fully discussed in an article [1]) especially devoted to that subject. Two methods of measuring have been particularly discussed, each of which allows of a fairly complete quantitative investigation of reverberation. In the meantime one of these methods, *viz.* that of exponential amplification, has been further developed and employed in a large number of tests. The present article describes the apparatus used and deals with some results obtained. First of all, we shall briefly outline once more the origin of reverberation, giving also the definition of reverberation time and dealing with the principle of the method of exponentially increasing amplification for measuring that time.

Let us imagine that a source of sound is active in one single frequency in an enclosed space during an indefinite length of time. A state of stability will then obtain. By this is understood the following: the sound pressure in the whole of the space as a function of time will be given by a sine function with the frequency of the source; the distribution of the sound pressure in space is a superposition of standing waves corresponding to the characteristic vibrations of the space in question. The shape and dimensions of the space determine what standing waves may occur in a given space. Which of these standing waves will be represented in the said superposition (in other words, which characteristic vibrations will be excited) and to what extent they will occur depends upon the frequency, the position and the shape of the source of sound. There will certainly not be present the standing waves which at the place where the sound source is situated (if this may be regarded as a point) would show a node. The fact that among the characteristic vibrations represented there will always be several yielding a considerable contribution towards the superposition is evident when one remembers (see the article quoted in footnote [1])) that the successive characteristic frequencies show very small differences.

After the source of sound is switched off the intensity of the sound of each of the characteristic vibrations excited will die out exponentially owing to absorption by the walls. This sound heard after switching off the source is called the reverberation. The sound pressure p will then be given as function of the time t by the equation:

$$p = p_0 \cdot e^{-k't} \cdot \sin(2\pi\nu_e t + \varphi); \quad . \quad . \quad (1)$$

where p_0 is the amplitude of the sound pressure before the sound source is switched off, k' is a constant which increases with the absorption by the walls, ν_e is the characteristic frequency in question and φ is a phase angle the magnitude of which depends upon the moment of switching off.

The reverberation time t_{60} is defined as the time it takes for the sound intensity to drop 60 db, *i.e.* by a factor 10^6. Now this intensity is proportional to the square of the amplitude of the sound pressure. From equation (1) it therefore follows that

$$10^{-3} = e^{-k't_{60}},$$

or

$$t_{60} = \frac{6.9}{k'} \quad . \quad . \quad . \quad . \quad . \quad . \quad . \quad . \quad . \quad (2)$$

[1]) W. Tak, The measurement of reverberation, Philips Techn. Rev. **8**, 82-88, 1946 (No. 3).

One of the methods for measuring reverberation time, viz. that of exponentially increasing amplification, is based on the following principle. The voltage induced by the reverberation by means of a microphone is amplified by an amplification which increases with time according to e^{at}, where a has a known and variable positive value. The amplified voltage is observed with a cathode-ray oscillograph, on the screen of which a sinusoidal line is to be seen whose amplitude increases or decreases according as $a > k'$ or $a < k'$ (see fig. 8 of the article quoted in footnote [1])). By adjusting a so as to keep the said amplitude constant, thus by making a equal to k', one finds from equation (2) the reverberation time t_{60}. Generally the constant k' is a function of the frequency, as is also the reverberation time. In order to determine the acoustics of a space it is therefore necessary to carry out successive measurements with a series of frequencies in the audible range.

The foregoing applies for the hypothesis assumed in the beginning where a source of sound is acting with one single frequency for an indefinite length of time. Actually such a condition will seldom occur with speech or music. Rather one has to do with series of sound impulses varying in duration and frequency, these impulses being so short as to preclude a state of stability. In order to approximate the condition existing with speech or music, in such a way that reproducible results may be expected, one can proceed in various ways. For instance the frequency of the sound can be modulated, or else the sound can be made to consist of short impulses of a certain tone. Since we consider the latter to be the best imitation of music or speech we have employed sound impulses when carrying out our measurements. Owing to the large number of characteristic vibrations excited by every impulse and the beats between these vibrations, the shape of the oscillograms becomes very complicated. We shall revert to this in the discussion of the measuring results.

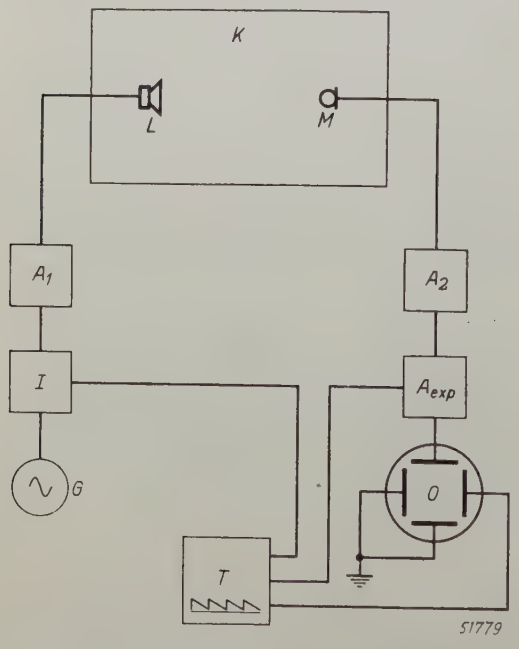

Fig. 1. In an enclosed space K where the reverberation time is to be measured a loudspeaker L and a microphone M are set up. The loudspeaker is connected *via* an amplifier A_1 and an impulse exciter I to a tone generator G. The microphone is connected to an oscillograph O *via* a pre-amplifier A_2 and an amplifier A_{exp} with exponentially increasing amplification. The generator T of the time-base voltage for the oscillograph also controls the impulse exciter and the exponential amplifier.

Description of the measuring apparatus

Fig. 1 shows diagrammatically of what components the measuring apparatus consists and how these are interconnected.

The microphone, set up in the space whose reverberation time is to be measured, is connected to a cathode-ray oscillograph via a pre-amplifier and the exponential amplifier to be discussed below. As source of sound a loudspeaker is used which is connected to a generator via an output amplifier and an impulse exciter, the latter serving to switch the loudspeaker on and off periodically so as to give a series of sound impulses.

Each sound impulse has to be synchronized with the beginning of the exponential amplification and the beginning of the movement of the luminous spot across the screen of the oscillograph from left to right. As soon as the amplification has reached its final value it has to return as quickly as possible to its initial value and the spot from the right side of the screen to the left side to start a new cycle.

What takes place is illustrated in *figs. 2a-d*, showing successively the sound intensity produced (I_L) and the sound intensity received (I_M), the logarithm of the amplification g of the exponential amplifier, and the horizontal deflection x on the oscillograph, all as functions of the time t. When the ratio of the final value g_T of the amplification to the initial value g_0 has been definitely adjusted so as to correspond to 60 db and the duration T of the cycle is so chosen that *the amplitude y of the oscillogram* (fig. 2e) *remains constant*, then T is the reverberation time t_{60} that is sought. Bearing in mind that the regulation of T practically means giving the right slope to the line $\ln g = \mathrm{f}(t)$ (fig. 2c), it is evident that the result is independent of both the duration of the impulse τ (fig. 2a) and the time t' (fig. 2b) the sound takes to travel the shortest path from the loudspeaker to the microphone.

If, for instance, t' is increased to t'' (fig. 2*b*) by setting up the microphone farther away from the loudspeaker, then the oscillogram will begin at t''

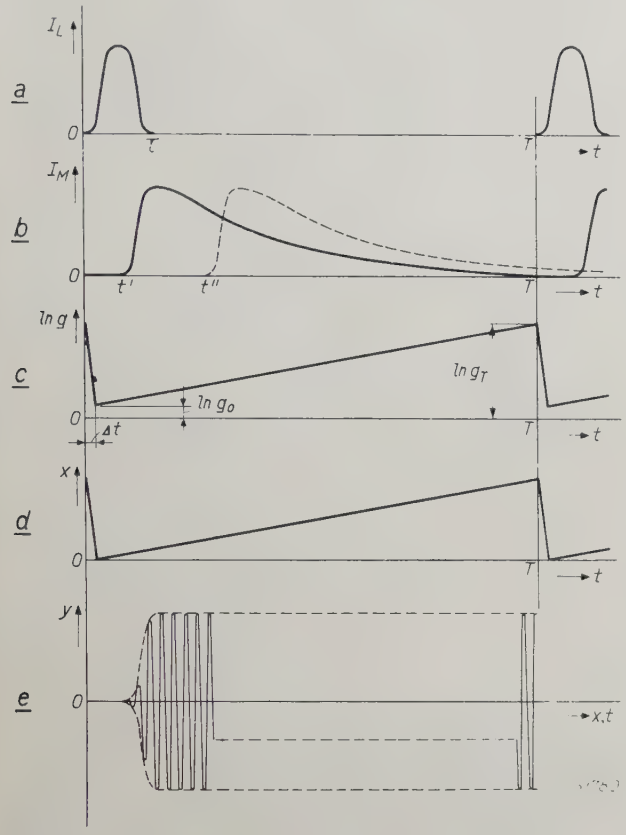

Fig.2.
a) The sound intensity I_L at the loudspeaker,
b) the sound intensity I_M at the microphone,
c) the logarithm of the amplification g of the exponential amplifier,
d) the horizontal deflection x and
e) the vertical deflection y on the oscillograph, all plotted as function of the time t.
T = duration of the cycle, τ = duration of the sound impulse, t', t'' = time required for the direct sound to travel from the loudspeaker to the microphone, Δt = time taken for the amplification of A_{exp} to return from the final value g_T to the initial value g_0.

but the same cycle T will be found during which the amplitude remains constant.

Only the interval Δt (fig. 2*c*) required by the amplifier to return from the final value to the initial value of amplification should be deducted from T, but this correction is so insignificant as to be negligible.

The aforementioned synchronization between the various phenomena is obtained by controlling from one point both the impulse exciter and the exponential amplifier and the horizontal deflection on the oscillograph. This central control point is the generator of the linear time-base voltage (T in fig. 1).

We shall now consider in succession this time-base voltage generator, the exponential amplifier and the impulse exciter.

The time-base voltage generator

In essence this consists of a capacitor gradually charged via a resistor from a direct voltage source E and rapidly discharging via a relay valve, the charging and discharging alternating periodically. The wiring diagram is given in *fig. 3* and explained in the text below it [2]). If the resistor through which the charge flows were an ordinary resistor then the capacitor voltage v_C would rise exponentially with t, but by using a pentode as resistor and causing it to work in the range where the anode current I_0 is independent of the anode voltage a constant charging current is obtained, so that $v_C = I_0 t/C_0$ changes linearly with t (C_0 = capacitance of the capacitor). The same applies for the voltage v_P on the pentode, $= E - I_0 t/C_0$.

The maximum amplitude of v_C is limited to a value which is a certain amount smaller than E; it depends in fact upon the striking voltage of the relay valve. With the aid of a variable direct voltage on the grid of the relay valve (see fig. 3) the striking voltage is so adjusted as to make the amplitude of v_C correspond to the voltage required to carry the luminous spot across the whole width of the screen of the oscillograph.

The period of the relaxation oscillation of the system described must, as we have seen, be equal to the reverberation time of the space under investigation. This reverberation time may be anything between about 0.1 sec (small, strongly damped room) and a number of seconds (large, cavernous spaces, *e.g.* a church.) The frequency of the relaxation oscillation must therefore be variable. Its cycle consists mainly of the charging interval of the capacitor, which is charged all the quicker

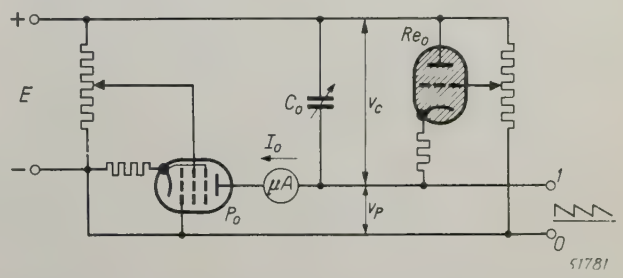

Fig. 3. Circuit for generating a linear time-base voltage (v_P). The capacitor C_0 is charged *via* the pentode P_0 with the anode current I_0, which is independent of the anode voltage, so that the voltage v_C on C_0 increases linearly with time. When v_C reaches the striking voltage of the relay valve Re_0 then C_0 discharges across Re_0 in a short time, after which it is charged again, and so on. The voltage $v_P = E - v_C$ is taken from the terminals *0-1*.

[2]) The same circuit is used for the time-base of the cathode-ray oscillograph type GM 3156 (see Philips Techn. Rev. **5**, 289-297, 1940). The lowest frequency obtainable with this oscillograph (1/4 c/s) is in many cases still too high for our purpose.

according as C_0 is smaller or I_0 is greater. In the practical construction of the apparatus these two quantities have been made adjustable: C_0 in coarse and fine stages, and I_0 continuously with the aid of the screen grid voltage of the pentode (see fig. 3). Before measuring is started the screen grid voltage is adjusted so that I_0 has a value fixed once for all. The actual measuring, i.e. making the vertical amplification, but, as will be seen from the following, this is neither necessary nor desirable.

Starting from the highest practicable intensity of the sound impulses, one finds in practice that after having been attenuated about 40 db the reverberation has already reached a level at which various interferences become troublesome. These interferences consist partly of the noise of the

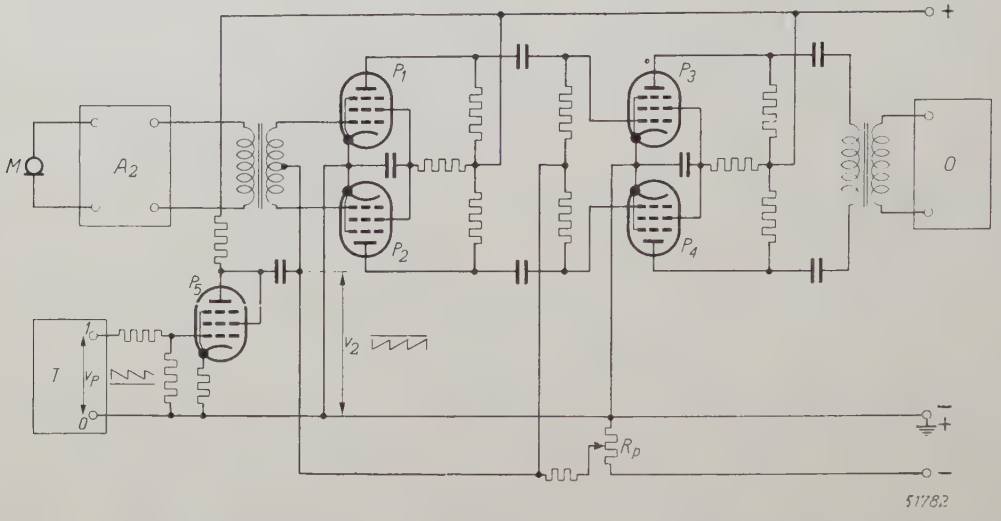

Fig. 4. Diagram of the exponential amplifier. The control grids of the two push-pull stages with the pentodes P_1-P_2 and P_3-P_4 receive a variable bias v_2 consisting of a fixed negative direct voltage derived from the potentiomenter R_P and a "sawtooth" voltage supplied by the pentode P_5. The control grid circuit of P_5 is connected via a voltage divider to the terminals *0-1* of the time-base voltage generator (fig. 3). The rest of the symbols have the same meaning as in fig. 1.

amplitude on the oscillograph constant, is done by regulating C_0.

The exponential amplifier

In the exponential amplifier pentodes are employed whose anode current in a certain range is an exponential function of the control grid voltage. When a certain range of this voltage is traversed linearly with time then the anode current — and likewise the mutual conductance — changes with time according to an exponential law. The same applies for the amplification factor of an amplifier in which such pentodes are used. Pentodes possessing this property are, for instance, those of the types EF 5 and EF 41.

Measurements taken on a push-pull amplifier with two stages equipped with these pentodes have shown that when the control grid voltage is changed simultaneously in both stages the limits of the range just mentioned correspond to values of the amplification lying about 50 db apart. The definition of reverberation time (t_{60}) is, it is true, based upon a fall of 60 db in the sound level, which should be compensated by an equally large increase in the amplifier and partly of sounds having nothing to do with the measurement. For this reason it is not desirable that the amplification should increase by more than 40 db. And this is in fact sufficient, since the time t_{40} in which the reverberation decreases 40 db in intensity is correlated in a simple manner to the time t_{60} that is sought:

$$t_{40} = \frac{2}{3} t_{60}.$$

(This may be seen at once, for instance, from fig. 7 of the article quoted in footnote [1]).) On the other hand it is not desirable to let the reverberation drop much less than 40 db, because then in the conversion to t_{60} the inevitable measuring errors would be increased by too large a factor.

We therefore decided to work upon a drop of 40 db in the reverberation and consequently an increase of 40 db in the amplification. With the abovementioned two-stage push-pull amplifier this increase of 40 db is obtained by causing the negative grid voltage to drop by about 32 V. To ensure that the amplification starts and stops at the right moments the grid voltage variation is brought

about by means of the time-base voltage generator. How this is done is shown in *fig. 4*. This generator supplies to terminal *1* a voltage which is highly positive with respect to terminal *0* (earth) and which gradually drops to a lower positive value. On the control grids of the pentodes $P_1 \ldots P_4$ in the exponential amplifier on the other hand a voltage is required (v_2, fig. 4) which rises from a highly negative to a less negative value. In order to derive the second voltage variation from the first one (v_P, fig. 4) a valve P_5 is introduced whose output voltage is superposed upon a direct voltage drawn from a potentiometer R_P; this sum (v_2) serves as a grid bias for $P_1 \ldots P_4$. The amplitude of v_2 and the direct voltage referred to are so chosen as to give the amplification variation of 40 db; to make sure that this remains so, the feeding voltages have to be carefully stabilized.

It is to be added that the frequency characteristic of the amplifier is a horizontal straight line in the audible range of about 50-10 000 c/s.

The impulse exciter

The impulse exciter is in fact an amplifying stage introduced between the tone generator and the final-stage amplifier (see fig. 1) and biassed in such a way as to be alternately either blocked or caused to act as an amplifier, so that the loudspeaker produces a series of sound impulses.

This varying bias is likewise drawn from the time-base voltage generator, so that the rhythm of the sound impulses corresponds to the frequency of the time-base voltage. This time-base voltage is first subjected to a certain distortion so as to satisfy the requirement of being able to regulate the duration of each impulse (τ, fig. 2*a*) within certain limits, and preferably without changing the maximum sound intensity. This requirement is made for the following reason.

A long impulse (of the order of the reverberation time) is undesirable, because during that time no reverberation can be observed and the width on the oscillograph screen corresponding to τ is therefore lost; τ must consequently be kept small with respect to the reverberation time. On the other hand very short impulses would not give sufficient volume of sound, particularly in large halls. The most favourable compromise must therefore be found.

The circuit applied by us, which answers these requirements, is represented in *fig. 5*. The resistor R_1, the capacitor C_1 and the relay valve Re_1 form a circuit which under the influence of the time-base voltage v_P produces a relaxation oscillation with the same frequency as that of v_P. The voltage on C_1 has a trend analogous to that of v_P but in the reverse sense (obliquely rising instead of falling "saw-teeth") and controls a pentode P_8. In the anode circuit of P_8 is a filter consisting of a system

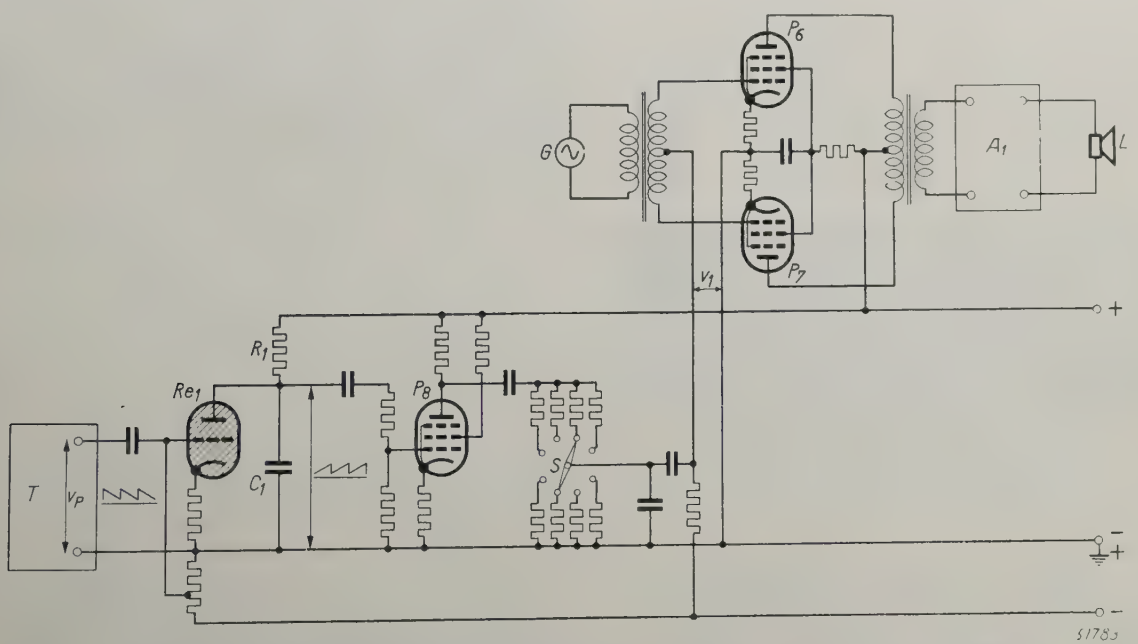

Fig. 5. Circuit diagram of the impulse exciter. The voltage v_P of the time-base voltage generator T (fig. 3) controls a relaxation oscillation in the circuit formed by the resistor R_1, the capacitor C_1 and the relay valve Re_1. The sawtooth voltage on C_1 is amplified by the pentode P_8 and distorted in a filter of capacitors and resistors into a periodical impulse which together with a fixed negative direct voltage forms the bias v_1 of a push-pull amplifier with the pentodes P_6 and P_7. The impulse width and thus also the time during which the amplifier is active are regulated by means of the switch S. For the rest of the symbols see fig. 1.

of capacitors and (partly variable) resistors. The output voltage of this filter system together with a fixed direct voltage forms the bias v_1 of the impulse exciter proper. The variation of v_1 with time is shown in *fig. 6* for the two extreme positions of the switch S indicated in fig. 5. It is seen that a more or less rounded off voltage impulse arises which during a time variable between τ_{min} and τ_{max}

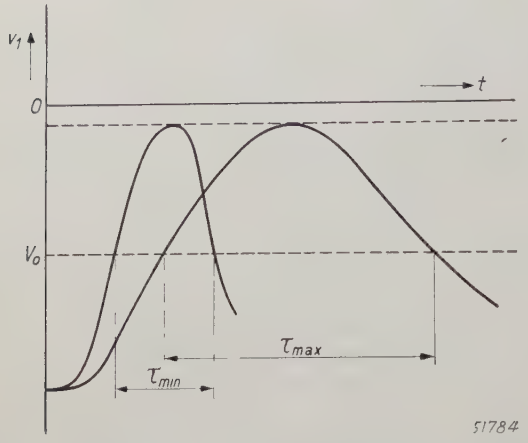

Fig. 6. Trend of the bias v_1 generated in the system of fig. 5 The time during which this bias exceeds the grid voltage V_0 at which the valves P_6 and P_7 (fig. 5) are blocked is variable between τ_{min} and τ_{max}.

exceeds the voltage V_0 at which the impulse exciter is blocked. The amplitude of the amount by which the impulse v_1 exceeds the value V_0 is practically independent of the position of the switch; this amount determines the amplification of the impulse exciter and thus ultimately the maximum sound intensity. This satisfies the requirement that sound impulses should be produced with a variable duration without affecting the maximum intensity.

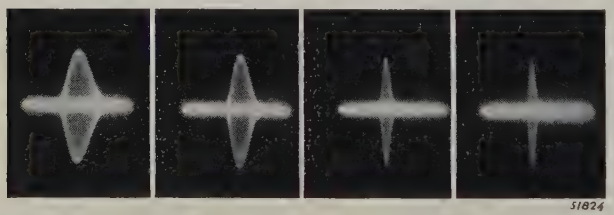

Fig. 7. Oscillograms of sound impulses obtained with the system according to fig. 5. The duration of the impulses is respectively 0.12, 0.07, 0.035 and 0.02 seconds.

Fig. 7. shows the oscillograms of sound impulses with a duration of 0.12, 0.07, 0.035 and 0.02 seconds.

Practical construction of the apparatus

The arrangement given diagrammatically in fig. 1 may consist partly of a number of normal apparatuses, viz. the tone generator, the final-stage amplifier, the oscillograph, the pre-amplifier and further the loudspeaker and the microphone. Except for the two last-mentioned components and the pre-amplifier, the others are mounted on a mobile rack (*fig. 8*) which also carries a cabinet containing the time-base voltage generator, the exponential amplifier and the impulse exciter. A separate cabinet contains the apparatus required for supplying the various components with stabilized direct voltages [3]). Finally there is an auxiliary oscillograph on which a Lissajous figure can be produced by the voltage from the tone generator and the a.c. mains. This makes it easy to adjust the tone frequency exactly to a multiple of the mains frequency, and if the latter may be regarded as constant then one is sure that the same frequency has been used when taking the various measurements, so that the results may be more comparable.

A measurment is carried out in the following way. When the apparatus described has been started up and the tone frequency given the desired value, the capacitance C_0 in the time-base voltage generator (fig. 3) is regulated so as to keep the amplitude of the oscillogram as nearly constant as possible. When this has been done the duration of the reverberation can be read from the position of the controls for regulating C_0.

Measuring results

Obviously when it comes to practical application matters will not be so simple as they have just been outlined above, considering that an enclosed space has a large number of characteristic vibrations all of which are more or less excited by the sound impulses and beats will arise between those vibrations. (Experimental confirmation of this will be referred to later on.) The picture on the oscillograph will never have such a simple shape as that shown in fig. 2*e*, but will always show a number of peaks. It will be seldom that an adjustment can be found to give peaks of equal size, but after some experience there will be no doubt about what is the best adjustment. For instance *figs 9a, b* and *c* are recordings taken under identical conditions with T values of 1.3, 1.1 and 0.9 second respectively, and there the best adjustment is $T = 1.1$ second.

Of course it is more difficult in cases where one has to do with two or more average reverberation times, as occurs for instance when a "soft" room (with short reverberation) is in communication *via* an open door with a "hard" corridor (long

[3]) H. J. Lindenhovius and H. Rinia, A direct current supply apparatus with stabilised voltage, Philips Techn. Rev. **6**, 54-61, 1941.

reverberation). *Fig. 10* shows two recordings made in such a case.

Finally a description is given of an experiment confirming the fact that sound impulses excite a series of characteristic vibrations of the room in which they are produced and that beats arise between those vibrations, as mentioned in the foregoing and in the article quoted in footnote [1]). The apparatus used in this experiment was the same as that previously described.

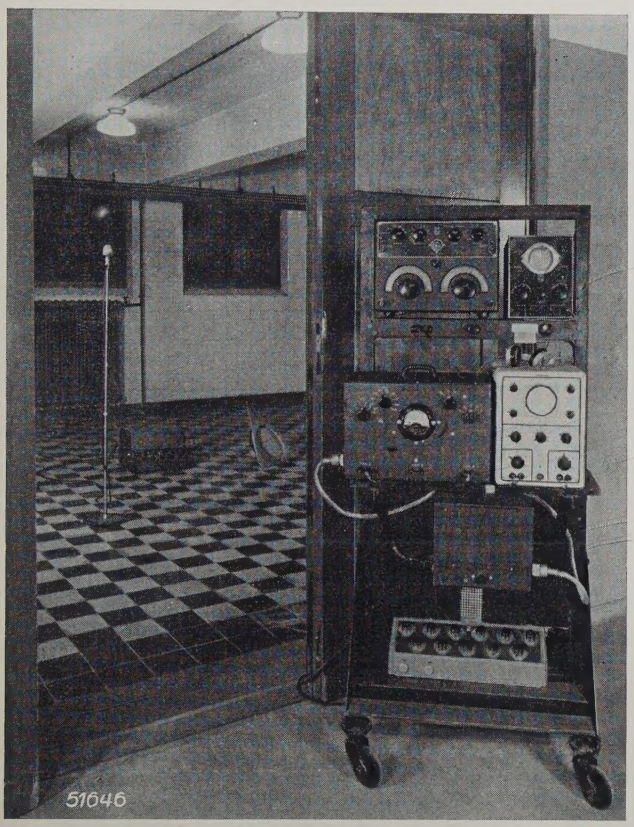

Fig. 8. Arrangement of the measuring apparatus. The mobile rack carries the following apparatus:

Top row: to the left the tone generator (type GM 2307), to the right an auxiliary oscillograph (type GM 3153) for adjusting the tone frequency to a multiple of the mains frequency.

Second row: to the left a cabinet containing the time-base voltage generator, the exponential amplifier and the impulse exciter; to the right the oscillograph (type GM 3159); underneath this the supply apparatus for the stabilized direct voltages.

At the bottom: the 24 W output amplifier (type 2843).

In the background in the room where the reverberation time is being measured are the microphone, the pre-amplifier (type 2843) and the loudspeaker.

First the impulse exciter was put out of action, so that the loudspeaker produced an uninterrupted note. Also the exponential amplifier was temporarily out of action; a constant amplification was applied between the microphone and the oscillograph tube. This tube received no voltage for the horizontal deflection, so that the image consisted only of a small vertical line the length of which

a *b* *c*

Fig. 9. Since there are always a number of characteristic vibrations excited simultaneously, the oscillogram does not show the simple form of fig. 2*e*, but has a number of peaks and valleys which make it difficult to find the right adjustment. Recordings have been made, under otherwise the same conditions, with T = (*a*) 1.3 sec, (*b*) 1.1 sec, (*c*) 0.9 sec. The adtustment (*b*) is the best.

j

was proportional to the sound pressure at the microphone. This line was photographed on a continuously moving film, whilst the frequency of the tone generator was gradually changed. The result was a picture of the sound pressure (at the microphone) as a function of the frequency (*fig. 11*). The frequency scale was fixed by interrupting the pick-up circuit every time a certain frequency was passed.

Fig. 11 shows that in the room where the experiment was carried out and with a given arrangement of loudspeaker and microphone few pronounced characteristic frequencies occur in the range between 1020 and about 1065 c/s, but that they do decidedly occur between about 1065 and 1120 c/s.

What conclusions are therefore to be drawn from this regarding the reverberation that will occur when sound impulses are produced in this room with different pitches within the frequency range traversed in this experiment and with different durations of the impulses?

Let us first give the tone a frequency equal to a characteristic frequency of the room lying roughly midway between two adjacent characteristic frequencies, for example 1072 c/s (see fig. 11). It may

a *b*

Fig. 10. Reverberation in a room communicating with a corridor through an open door. (*a*) was recorded with T = 0.9 sec, (*b*) under otherwise the same conditions but with T = 2.3 sec. In the case of (*a*) the speed of the amplification practically balances with the expiration of the reverberation in the room but not with the slower expiration in the corridor. It is seen that after some time the deflection increases, due to predominance of the reverberation in the corridor. In the case of (*b*) T was so chosen as to obtain a practically constant amplitude of the reverberation in the corridor. Here, too, there is an increase of amplitude towards the end, but this is due to the noise of the amplifier.

then be expected that this characteristic frequency as well as the two adjacent ones (1069 and 1076 c/s) will be strongly excited, whilst more remote vibrations (*e.g.* 1085 c/s) will be much less excited, and that beats will arise with a frequency that is the difference between the note frequency and that of the first-mentioned vibrations (3-4 c/s).

This is confirmed by *fig. 12a*, recorded with the whole of the measuring apparatus described in this article in action, thus including impulse exciter, exponential amplifier and time-base. Here we see a more or less sinusoidal pressure amplitude varying with time and showing exactly two cycles in the time-base period. In this experiment the time-base period was 0.54 second, so that the frequency of the amplitude variation was 2/0.54 = 3.7 c/s, which corresponds well with the frequency differences between the pitch used (1072 c/s) and the two adjacent characteristic frequencies. The phenomenon represented in fig. 12*a* may therefore be ascribed to beats between these frequencies.

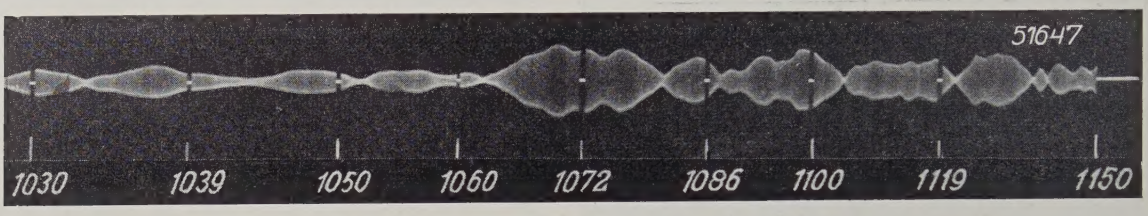

Fig. 11. Amplitude p_0 of the sound pressure at a point in a room as function of the frequency of a continuous note (in cycles per second).

If we now choose 1060 c/s as tone frequency then, as may be seen from fig. 11, the nearest pronounced characteristic frequencies are the same three as just mentioned (1069, 1072 and 1076 c/s). In the oscillogram of the reverberation (*fig. 13a*) we now recognize — though less clearly than in fig. 12*a* — a frequency of about 14 c/s, which again corresponds, within the accuracy of measurement of the frequencies, to the difference between the pitch used and the adjacent characteristic frequencies. The same is the case with a tone of 1086 c/s (*fig. 14a*), where according to fig. 11 one would expect excitation not only of the group around 1072 c/s but also of the characteristic frequencies at 1093 and 1100 c/s, and therefore, in the image of the reverberation, beat frequencies of 7 and 17 c/s, among others. These two interferences are indeed to be recognized in fig. 14*a*.

Figs 12*a*, 13*a* and 14*a* have all been recorded with a fairly long duration of the sound impulses, τ = 0.12 sec, so that each impulse covered more than 100 cycles. The images obtained with shorter impulses are given in the same figures above *b*, *c* and *d* where the values of τ were respectively 0.07, 0.035 and 0.02 sec. The shorter the duration of the impulses, the more complicated is the structure of the oscillograms, which points to a larger number of excited characteristic frequencies. This is not surprising considering that in the Fourier spectrum of the sound impulse more terms are involved according as the impulse is shorter.

A change of the impulse duration τ can therefore contribute towards giving the oscillogram such a shape as to make it easier to find the right adjustment of the period T. This was in fact another reason why τ was made variable.

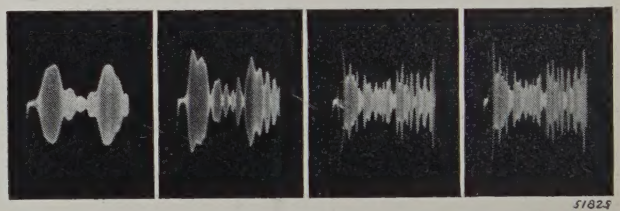

Fig. 12. Oscillograms recorded with the apparatus according to fig. 8. Duration of the sound impulses: (*a*) 0.12 sec., (*b*) 0.07 sec., (*c*) 0.035 sec., (*d*) 0.02 sec. Pitch 1072 c/s. The width of the oscillogram corresponds to 0.54 sec. Since it was not necessary in this case to adjust as accurately as possible the constant amplitude, this was only done approximately.

Fig. 13. The same as fig. 12 but with a tone of 1060 c/s.

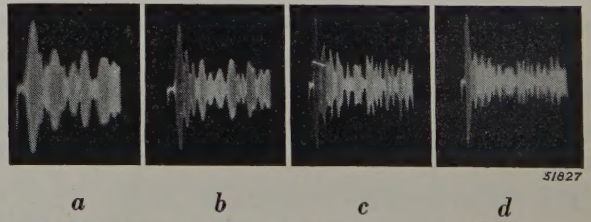

Fig. 14. The same as fig. 12 but with a tone of 1086 c/s.

ABSTRACTS OF RECENT SCIENTIFIC PUBLICATIONS OF THE N.V. PHILIPS' GLOEILAMPENFABRIEKEN

Reprints of the majority of these papers can be obtained on application to the Administration of the Research Laboratory, Kastanjelaan, Eindhoven, Netherlands. Those papers of which no reprints are available in sufficient number are marked with an asterik.

R 32: B. D. H. Tellegen: Coupled Circuits (Philips Res. Rep. **2**, 1-19, 1947 No. 1)

The theory of coupled circuits leads, in the determination of the frequencies and dampings of the free oscillations, to an equation of the fourth degree. If we confine ourselves to cases in which the resonance curve has a small relative width, that equation can be reduced to one of the second degree which can be resolved into factors in a simple manner. Each of the factors determines one of the free oscillations. Inductive or capacitive coupling leads to a real coupling factor k, resistance coupling to an imaginary k, mixed coupling to a complex k. If the circuits are equally damped and equally tuned, then, when k is real, the factors have equal dampings but different characteristic frequencies; when k is imaginary they have equal characteristic frequencies but different dampings; when k is complex they have both different characteristic frequencies and different dampings. If the circuits are equally damped but differently tuned the effect on the shape of the resonance curve is the same as that of an increase of k^2. If the circuits are equally tuned but unequally damped k^2 is apparently diminished. If the circuits are differently tuned and unequally damped k^2 is apparently altered by a complex amount. All symmetrical resonance curves can be drawn in a single family. The height of the resonance curve is also investigated. Finally, systems are considered in which the circuits are coupled over an arbitrary four-terminal network which may also contain an amplifying valve.

R 33: W. Elenbaas: On the excitation temperature, the gas temperature, and the electron temperature in the high-pressure mercury discharge. (Philips Res. Rep. **2**, 20-41, 1947, No. 1)

The excitation temperature of a high-pressure discharge, the temperature of which was formerly determined from the intensity decrease, perpendicularly to the axis, of spectral lines having different initial levels, is determined from the absolute value of the intensity of the yellow lines (5770/5791 Å) combined with the transition probability of these lines, as measured by Schouten and Smit. The temperature found by the last method is considerably lower than that previously determined. The cross section of the Hg atom which must be used in the Langevin equation in order to arrive at the right current (the density of the electrons being determined by the Saha equation), as well as the vapour pressure, are computed by assuming the excitation temperature to coincide a) with the gas temperature and b) with the electron temperature. In case b) we determine the gas temperature by assuming that the electrons deliver energy to the atoms through elastic collisions just sufficiently to compensate the loss by conduction of heat. In both cases we find for the cross section of the Hg atom a reasonable value, viz. 4.10^{-15} cm^2. The pressure as computed from the gas temperature and the mean vapour density agrees better with the measured value in the case b) than in the case a) (differences 2.5 and 8 per cent, respectively). In case b) one has to apply a correction to the temperature as formerly determined from the intensity decrease perpendicularly to the axis, resulting in a satisfactory agreement between the two methods. Finally, the excitation probability of the 3d and 3D levels from the ground level was estimated. The excitation by electron impact is much more frequent than the excitation by mutual collisions of the atoms, but yet it is far too small to explain temperature equilibrium.

R 34: H. B. G. Casimir: On the theory of eddy currents in ferromagnetic material (Philips Res. Rep. **2**, 42-54, 1947, No. 1)

The theory of eddy currents in ferromagnetic material is developed for the limiting case that the depth of penetration d is small, although the product μd is not necessarily small.

First the rigorous solution for the sphere is discussed for this limiting case. Next it is shown that the solution can be obtained from Laplace's equation with a new type of boundary condition. This boundary condition is then applied to a discussion of eddy currents in spheroids. Explicit formulae are found both for small and for very large values of $\mu d/R$

Special attention is given to the limits for very long and very flat spheroids.

R 35: H. C. Hamaker: Radiation and heat conduction in light-scattering material. I. Reflection and transmission. (Philips Res. Rep. 2, 55-67, 1947, No. 1)

On the basis of a set of simultaneous differential equations originally due to Schuster the transmission and reflection of light in light-scattering layers is discussed. Formulae previously developed by Kubelka and Munk are briefly recapitulated; they are extended so as to describe the luminescence of fluorescent screens excited by X-rays or electron bombardment. Likewise formulae are derived that include temperature radiation.

R 36: H. A. Klasens: The light emission from fluorescent screens irradiated by X-rays. (Philips Res. Rep. 2, 68-78, 1947, No. 1)

Applying Schuster's theory as extended by Hamaker for the scattering and absorption of light, general equations are deduced for the amount of light emitted by fluorescent screens irradiated by X-rays. Some commercial screens are examined to measure the "absorption" coefficient of the fluorescent light. Several means of increasing the brightness of a screen are discussed. (see Philips techn. Rev. 9, 364-370, 1947, No. 2)

R 37: J. L. Meyering and M. J. Druyvesteyn: Hardening of metals by internal oxidation I. (Philips Res. Rep. 2, 81-102, 1947, No. 2)

Alloys of silver, copper and nickel can be dispersion-hardened by diffusing oxygen into an alloy with e.g. 1—2 atomic % of an element having a sufficient affinity for O. Too small an affinity leads to a coarser distribution of the oxide formed, because conglomeration must take place via the atoms, and dissociation occurs more frequently when the oxide is not very stable. Thermodynamical considerations are given, and calculations of the penetration of the reaction front.

R 38: H. C. Hamaker: Radiation and heat conduction in light-scattering material. II. General equations including heat conduction. (Philips Res. Rep. 2, 103-111, 1947, No. 2)

The equations of Schuster describing the transmission of radiation through light-scattering material are now extended so as to include temperature radiation and heat conduction. Linearization leads to a system of three simultaneous linear differential equations, amongst which one of the second order. These are resolved and certain general features of the solution are discussed. In particular an expression is deduced for the energy transport due to radiation.

R 39: H. C. Hamaker: Radiation and heat conduction in light-scattering material. III Application of the theory. (Philips Res. Rep. 2, 112-125, 1947, No. 2).

The set of equations developed in the foregoing paper and describing the combined transmission of energy by radiation and by thermal conduction in light-scattering material are applied to practical problems. In the first place the boundary conditions at the surface of a thick layer are investigated. Near the surface the temperature is no longer a linear function of the distance from the surface. Formulae for the deviation from linearity are deduced and the order of magnitude of these deviations is indicated. On the basis of these theories it is pointed out that observations of the thermal conductivity of oxide cathodes by various authors are unreliable since they are founded on unjustifiable assumptions.

Application of the present theory to layers of finite thickness are only briefly discussed. On the whole the theory is a very crude one, so that it is not to be expected that detailed applications will be of great practical value.

R 40: A. van Weel: An improved method for coupling valves for ultrashort waves. (Philips Res. Rep. 2, 126-135, 1947, No. 2)

A method for coupling two electron valves or one valve with an antenna is described, by which method the difficulties due to the finite inductance of the internal electrode leads of a valve can be eliminated up to very high frequencies. In addition to this the new system provides a very simple way to realize matching of the valve impedances.

R 41: F. L. H. M. Stumpers: Interference problems in frequency modulation. (Philips Res. Rep. 2, 136-160, 1947, No. 2)

After a survey of definitions, the general problem of interference with frequency-modulated signals is treated. Special attention is paid to the pauses of the desired signal. The case of equal amplitudes gives rise to some interesting mathematical relations. The loudness level of disturbances is computed. In the last two sections the interference caused by synchronized transmitters (or by two-path transmission of one signal) is extensively dealt with. Many numerical examples illustrate the theory.